5-9-2002

Higher-Order Evaluation of the Critical Temperature For Interacting Homogeneous Dilute Bose Gases

Frederico F. F. de Souza Cruz
Federal University of Santa Catarina

Marcus Pinto
Federal University of Santa Catarina

Rudnei O. Ramos
Dartmouth College

Paulo Sena
Federal University of Santa Catarina

In press Physical Review A (2002)

Higher Order Evaluation of the Critical Temperature for Interacting Homogeneous Dilute Bose Gases

Frederico F. de Souza Cruz,[1,*] Marcus B. Pinto,[1,2,†] Rudnei O. Ramos,[3,4,‡] and Paulo Sena[1,5,§]

[1] *Departamento de Física, Universidade Federal de Santa Catarina, 88040-900 Florianópolis, SC, Brazil*
[2] *Laboratoire de Physique Mathématique et Théorique - CNRS - UMR 5825 Université Montpellier II, France*
[3] *Departamento de Física Teórica, Universidade do Estado do Rio de Janeiro, 20550-013 Rio de Janeiro, RJ, Brazil*
[4] *Department of Physics and Astronomy, Dartmouth College, Hanover, New Hampshire 03755-3528*
[5] *Universidade do Sul de Santa Catarina, Av. José A. Moreira, 787, 88704-900 Tubarão, SC, Brazil*

We use the nonperturbative linear δ expansion method to evaluate analytically the coefficients c_1 and c_2'' which appear in the expansion for the transition temperature for a dilute, homogeneous, three dimensional Bose gas given by $T_c = T_0\{1+c_1 an^{1/3}+[c_2' \ln(an^{1/3})+c_2'']a^2n^{2/3}+\mathcal{O}(a^3n)\}$, where T_0 is the result for an ideal gas, a is the s-wave scattering length and n is the number density. In a previous work the same method has been used to evaluate c_1 to order-δ^2 with the result $c_1 = 3.06$. Here, we push the calculation to the next two orders obtaining $c_1 = 2.45$ at order-δ^3 and $c_1 = 1.48$ at order-δ^4. Analysing the topology of the graphs involved we discuss how our results relate to other nonperturbative analytical methods such as the self-consistent resummation and the $1/N$ approximations. At the same orders we obtain $c_2'' = 101.4$, $c_2'' = 98.2$ and $c_2'' = 82.9$. Our analytical results seem to support the recent Monte Carlo estimates $c_1 = 1.32 \pm 0.02$ and $c_2'' = 75.7 \pm 0.4$.

PACS numbers: 03.75.Fi, 05.30.Jp, 11.10.Wx

I. INTRODUCTION

Recently, the evaluation of the critical temperature for interacting dilute homogeneous Bose gases has been the interest of many theoretical works. For this purpose, the starting model is the one used in the analysis of a gas of interacting boson particles, described by a complex scalar field ψ, with a local interaction characterized by the s-wave scattering length a and Euclidean action which, in natural unities, can be written as

$$S_E = \int_0^\beta d\tau \int d^3x \left\{ \psi^*(\mathbf{x},\tau) \left(\frac{d}{d\tau} - \frac{1}{2m}\nabla^2 \right) \psi(\mathbf{x},\tau) - \mu\psi^*(\mathbf{x},\tau)\psi(\mathbf{x},\tau) + \frac{2\pi a}{m} \left[\psi(\mathbf{x},\tau)\psi^*(\mathbf{x},\tau)\right]^2 \right\} . \tag{1.1}$$

The field ψ can be decomposed into imaginary-time frequency modes $\psi_j(\mathbf{x},\omega_j)$, with discrete Matsubara frequencies $\omega_j = 2\pi j/\beta$ and j being an integer whereas β is the inverse of the temperature. At the early stages of solving this problem [1] the non-zero Matsubara frequency modes have been integrated out generating a reduced three dimensional $O(2)$ scalar theory. This procedure was justified on the grounds that near the transition the non-zero Matsubara modes decouple and one is left with an effective action given by

$$S_{3d} = \beta \int d^3x \left\{ \psi_0^* \left(-\frac{1}{2m}\nabla^2 - \mu \right) \psi_0 + \frac{2\pi a}{m} \left[\psi_0\psi_0^*\right]^2 \right\} . \tag{1.2}$$

Despite this simplification the problem remains non-trivial since ordinary perturbation theory cannot be used to treat the model at the phase transition due to the severe infrared divergences for the zero frequency modes ψ_0 at the critical point, originating the breakdown of conventional perturbation theory. Different nonperturbative methods, some of which are currently used in quantum field theories, have then been used to compute the transition temperature. The analytical methods include the self-consistent resummation (SCR) used by the authors of Ref. [1], the $1/N$ expansion

*Electronic address: fred@fsc.ufsc.br
†Electronic address: marcus@lpm.univ-montp2.fr; [1] Permanent address
‡Electronic address: rudnei@dft.if.uerj.br; [3] Permanent address
§Electronic address: psena@bon.matrix.com.br; [5] Permanent address

used at leading order ($1/N$-LO) by Baym, Blaizot and Zinn-Justin [2] and at next to leading order ($1/N$-NLO) by Arnold and Tomásik [3] as well as the linear δ-expansion (LDE) employed by some of the present authors in Ref. [4]. The numerical methods used mainly Monte Carlo lattice simulations (MCLS) like the ones employed recently by Arnold and Moore [5] and by Karshunikov, Prokof'ev and Svistunov [6]. Most of those calculations predicted that, in the dilute limit, the shift of the critical temperature of the interacting gas, T_c, as compared to the critical temperature for an ideal gas, T_0, $\Delta T_c = T_c - T_0$, behaves as

$$\frac{\Delta T_c}{T_0} = c_1 a n^{1/3} + \mathcal{O}\left(a^2 n^{2/3}\right) \ , \tag{1.3}$$

where n is the number density, c_1 is a numerical constant and the critical temperature for an ideal gas is given as usual by

$$T_0 = \frac{2\pi}{m}\left[\frac{n}{\zeta(3/2)}\right]^{\frac{2}{3}} \ . \tag{1.4}$$

The constant c_1 in Eq. (1.3) is directly related to the contributions from the zero mode Matsubara frequencies and therefore can only be computed from nonperturbative methods. Some recent numerical applications predicted values for c_1 which are close to 1.30 (MCLS, [5, 6]). On the other hand, the analytical applications mentioned above predicted the values 2.90 (SCR, [1]), 2.33 ($1/N$-LO, [2]), 1.71 ($1/N$-NLO, [3]) and 3.06 (LDE, [4]). Additionally, the authors of Ref. [7] have also argued that a logarithmic term appears at order-a^2 in Eq. (1.3). They have shown that this term is of the form $c_2' a^2 n^{2/3} \ln(a n^{1/3})$ and also estimated, using large-N arguments, the value of the numerical coefficient c_2'. Recently, Arnold, Moore and Tomásik [8] have argued that when naively going from the original action (S_E) to the reduced action (S_{3d}) by ignoring the effects of non-zero frequency modes one misses the effects that short-distances and/or high-frequency modes have on long-distance physics. For $T_c(n)$ at second order these effects can be absorbed into a modification of the strengths of the relevant interactions which means that one should consider the more general form for the reduced effective action Eq. (1.2)

$$S_{\rm eff}[\psi_0, \psi_0^*] = \beta \int d^3x \left\{ \psi_0^* \left(-\mathcal{Z}_\psi \frac{1}{2m}\nabla^2 - \mu_3 \right) \psi_0 + \mathcal{Z}_a \frac{2\pi a}{m} \left[\psi_0^* \psi_0\right]^2 + \mathcal{O}\left[\psi_0^* \psi_0 |\nabla\psi|^2, (\psi^*\psi)^3\right] \right\} + \beta F_{\rm vacuum} \ , \tag{1.5}$$

where $\mathcal{Z}_\psi$ is the wave-function normalization function, μ_3 incorporates the mass renormalization function, $\mathcal{Z}_a$ incorporates the vertex renormalization function and $F_{\rm vacuum}$ represents the vacuum energy contributions coming from the integration over the nonstatic Matsubara modes. The $\mathcal{O}\left[\psi_0^*\psi_0|\nabla\psi_0|^2, (\psi_0^*\psi_0)^3\right]$ terms represent higher order interactions in the zero modes of the fields. As emphasized in Ref. [8], these terms will give contributions to the density of order a^3 and higher and therefore do not enter in the order-a^2 calculations. By matching perturbative order-a^2 results obtained with the original action S_E and the general effective action $S_{\rm eff}$, the authors of Ref. [8] were able to show that the transition temperature for a dilute, homogeneous, three dimensional Bose gas can be expressed at next to leading order as

$$\frac{\Delta T_c}{T_0} = c_1 a n^{1/3} + \left[c_2' \ln(a n^{1/3}) + c_2''\right] a^2 n^{2/3} + \mathcal{O}\left(a^3 n\right) \ . \tag{1.6}$$

A similar structure is also discussed in Ref. [9]. As far the numerical coefficients are concerned, the *exact* value for c_2', $c_2' = -64\pi\zeta(1/2)\zeta(3/2)^{-5/3}/3 \simeq 19.7518$, was obtained using perturbation theory [8]. The other two coefficients cannot be obtained perturbatively but they can, through the matching calculation, be expressed in terms of the two nonperturbative quantities κ and $\mathcal{R}$ which are, respectively, related to the number density $\langle\psi_0^*\psi_0\rangle$ and to the critical chemical potential μ_c, as shown below. The actual relation in between the two nonperturbative coefficients and these physical quantities is given by [8]

$$c_1 = -128\pi^3 [\zeta(3/2)]^{-4/3} \kappa \ , \tag{1.7}$$

and

$$c_2'' = -\frac{2}{3}[\zeta(3/2)]^{-5/3} b_2'' + \frac{7}{9}[\zeta(3/2)]^{-8/3}(192\pi^3\kappa)^2 + \frac{64\pi}{9}\zeta(1/2)[\zeta(3/2)]^{-5/3}\ln\zeta(3/2) \ , \tag{1.8}$$

where b_2'' in Eq. (1.8) is given by

$$b_2'' = 32\pi \left\{ \left[\frac{1}{2} \ln(128\pi^3) + \frac{1}{2} - 72\pi^2\mathcal{R} - 96\pi^2\kappa \right] \zeta(1/2) + \frac{\sqrt{\pi}}{2} - K_2 - \frac{\ln 2}{2\sqrt{\pi}} \left[\zeta(1/2)\right]^2 \right\} , \tag{1.9}$$

with $K_2 = -0.13508335373$. The quantities κ and $\mathcal{R}$ are related to the zero Matsubara modes only. Therefore, they can be nonperturbatively computed directly from the reduced action $S_{\rm eff}$ which, as discussed in the numerous previous applications, can be written as

$$S_\phi = \int d^3x \left[\frac{1}{2} |\nabla\phi|^2 + \frac{1}{2} r_{\rm bare}\phi^2 + \frac{u}{4!}(\phi^2)^2 \right] , \tag{1.10}$$

where $\phi = (\phi_1, \phi_2)$ is related to the original real components of ψ_0 by $\psi_0(\mathbf{x}) = \sqrt{mT/\mathcal{Z}_\psi}\, [\phi_1(\mathbf{x}) + i\phi_2(\mathbf{x})]$, $r_{\rm bare} = -2m\mu_3/\mathcal{Z}_\psi$ and $u = 48\pi amT(\mathcal{Z}_a/{\mathcal{Z}_\psi}^2)$. The vacuum contribution appearing in Eq. (1.5) will not enter in the specific calculation we do here.

The three dimensional effective theory described by Eq. (1.10) is super renormalizable [1] requiring only a mass counterterm to eliminate any ultraviolet divergence. In terms of Eq. (1.10), the quantities κ and $\mathcal{R}$ appearing in Eqs. (1.7) - (1.9) are defined by [8]

$$\kappa \equiv \frac{\Delta\langle\phi^2\rangle_c}{u} = \frac{\langle\phi^2\rangle_u - \langle\phi^2\rangle_0}{u} , \tag{1.11}$$

and

$$\mathcal{R} \equiv \frac{r_c}{u^2} = -\frac{\Sigma(0)}{u^2} , \tag{1.12}$$

where the subscripts u and 0 in Eq. (1.11) mean that the density is to be evaluated in the presence of interactions and in the absence of interactions, respectively, and $\Sigma(0)$ is the self-energy with zero external momentum. Since they dependent on the zero modes their evaluation is valid, at the critical point, only when done in a nonperturbative fashion. As discussed in the next section the relation between r_c and $\Sigma(0)$ comes from the Hugenholtz-Pines theorem at the critical point.

Eq. (1.6) is a general order-a^2 result with coefficients that, therefore, depend on nonperturbative physics via κ and $\mathcal{R}$. In principle, to evaluate these two quantities one may start from the effective three-dimensional theory, given by Eq. (1.10), and then employ any nonperturbative analytical or numerical technique. In general, the analytical nonperturbative methods give a prescription so as to select and sum an *infinite* number of contributions belonging to a given class. For example, the infinite subset that contains only direct (tadpole) contributions represents the Hartree approximation, whereas exchange contributions are also taken into account in the Hartree-Fock approximation. In practice the sum is achieved by using a modified ("dressed") propagator to evaluate physical quantities. The nonperturbative results are then generated by solving self-consistent equations. However, in resumming calculations the bookkeeping and renormalization may become a problem beyond leading orders.

Another popular analytical nonperturbative technique is the $1/N$ expansion [10, 11] where one sums infinite subsets of contributions whose order is labeled by $\mathcal{O}(1/N^n)$ where N is the number of field components. In general, the leading order contribution is easily evaluated and may reveal interesting nonperturbative physics, at least from a qualitative point of view, apart for providing an "exact" result within the large-N limit. A nice illustration is provided by its application, for example, to the Gross-Neveu model at zero temperature, where the issue of chiral symmetry breaking as well as asymptotic freedom were investigated [12]. From a quantitative point of view the leading order may not be sufficient and lead to errors since N is finite and not too large in most cases. An example of this case is illustrated by treating the same Gross-Neveu model at finite temperature, where the leading order large-N calculation predicts a finite value for the critical temperature at which chiral symmetry restoration takes place, in contradiction to Landau's theorem for phase transitions in one space dimension [13].

In practice, going to higher orders can be a difficult task. Nevertheless, the $1/N$ ranks as a good method to investigate nonperturbative physics as shown in many applications. In particular, the results provided by this approximation

---

[1] Recall that the coupling constant, u, has dimensions of mass in natural unities.

for the interacting Bose gas case, where $N = 2$, are surprisingly good already at leading order [2]. Good numerical results can also be obtained with self-consistent methods despite some potential problems as discussed in Ref. [9]. The numerical calculations use mainly Monte Carlo lattice techniques and many different results, for the interacting Bose gas critical temperature problem, were generated in this way. The differences arise mainly from the way the theory is put on the lattice, the size of the lattice, the way the continuum limit is taken and other issues. As already mentioned, two recent works seem to have settled this question [5, 6].

Here we shall present, and then apply, an alternative analytical nonperturbative method known as the linear δ expansion (LDE) [14, 15] (for earlier works, see for instance, Ref. [16]), which is closely related to the variational perturbation theory [17] and the Gaussian effective potential [18]. This same method re-appeared under the name of optimized perturbation theory [19]. The main attractive feature of this approximation is the fact that the actual evaluation of a physical quantity, including the selection of the *finite* subset of relevant contributions at each order, is done exactly as in perturbation theory. It is then easy to control and explicitly evaluate one by one each of the reduced number of contributions appearing at each order. The implementation of the renormalization procedure follows the one performed in most quantum field theory textbooks [20]. After the usual perturbative manipulation one generates nonperturbative results through an optimization procedure, as we will discuss in the next section.

This work is organized as follows. In Sec. II we present the method and illustrate it with a simple application to the pure anharmonic oscillator. In the same section we implement the method in the effective three dimensional theory given by Eq. (1.10) in order to evaluate the constants κ and $\mathcal{R}$, Eqs. (1.11) and (1.12). The quantity r_c is then evaluated in Sec. III whereas $\langle\phi^2\rangle$ is evaluated in Sec. IV. The optimization procedure is carried out in Sec. V where the numerical results are presented and compared with some of the recent results. We present our conclusions in Sec. VI. All contributions, which include difficult five-loop Feynman diagrams with arbitrary N, are explicitly evaluated by brute force without recurring to any approximations. An appendix is included to show the details of the calculations of these higher order terms. To our knowledge, some of them have not been evaluated in this way before.

II. THE METHOD AND ITS APPLICATION TO THE INTERACTING BOSE GAS PROBLEM

A. The linear δ expansion

The linear δ expansion (LDE) was conceived to treat nonperturbative physics while staying within the familiar calculational framework provided by perturbation theory. In practice, this can be achieved as follows. Starting from an action S one performs the following interpolation

$$S \to S_\delta = \delta S + (1-\delta)S_0(\eta)\ , \tag{2.1}$$

which reminds the trick consisting of adding and subtracting a mass term to the original action. One can readily see that at $\delta = 1$ the original theory is retrieved. This parameter is really just a bookkeeping parameter and some authors do not even bother considering it explicitly as we do [21]. The important modification is encoded in the field dependent quadratic term $S_0(\eta)$ that, for dimensional reasons, must include terms with mass dimensions (η). In principle, one is free so as to choose these mass terms and within the Hartree approximation they are replaced by a direct (or tadpole) type of self-energy before one performs any calculation. In the LDE they are taken as being completely arbitrary mass parameters which will be fixed at the very end of a particular evaluation. One then formally pretends that δ labels interactions so that S_0 is absorbed in the propagator whereas δS_0 is regarded as a quadratic interaction. So, one sees that the physical essence of the method is the traditional dressing of the propagator to be used in the evaluation of physical quantities very much as in the Hartree case. What is different in between the two methods is that with the LDE the propagator is completely arbitrary while it is constrained to cope only with direct terms within the Hartree approximation. So, within the latter approximation the relevant contributions are selected according to their topology from the start.

Within the LDE one calculates in powers of δ as if it was small. In this aspect the LDE resembles the large-N calculation since both methods use a bookkeeping parameter which is not a physical parameter like the original coupling constants and within each method one performs the calculations formally working as if $N \to \infty$ or $\delta \to 0$, respectively. Finally, in both cases the bookkeeping parameters are set to their original values at the end which, in our case, means $\delta = 1$. However, quantities evaluated with the LDE dressed propagator will depend on η unless one could perform a calculation to all orders. Up to this stage the results remain strictly perturbative and very similar to the ones which would be obtained via a true perturbative calculation. It is now that the freedom in fixing η generates nonperturbative results. Since η does not belong to the original theory one requires that a physical quantity Φ calculated with the LDE be evaluated at the point where it is less sensitive to this parameter. This criterion, known as the Principle of Minimal Sensitivity (PMS), translates into the variational relation [18]

$$\frac{d\Phi}{d\eta}\Big|_{\bar{\eta}} = 0 \; . \tag{2.2}$$

The optimum value $\bar{\eta}$ which satisfies Eq. (2.2) must be a function of the original parameters including the couplings, which generates the nonperturbative results. The convergence properties of this method has been rigorously proved in the context of the anharmonic oscillator (AO) [21, 22, 23, 24]. Very recently, Kneur and Reynaud [25] claimed to have proved the convergence of this method in renormalizable quantum field theories. These are very encouraging results for the present application which uses a renormalizable effective model which shares many similarities with the pure AO. Let us quickly illustrate how this method works by considering the anharmonic oscillator described, in Minkowski space, by

$$\mathcal{L} = \frac{1}{2}(\partial_0\phi)^2 - \frac{1}{2}m^2\phi^2 - \frac{\lambda}{4}\phi^4 \; . \tag{2.3}$$

If one sets $m = 0$ in the relation above the model describes the pure anharmonic oscillator which cannot be treated by usual perturbation theory. Let us first consider the ground state energy density whose exact result, $\mathcal{E}^{\rm exact} = \lambda^{1/3}0.420804974478\ldots$, has been calculated by Bender, Olaussen and Wang [26]. Following Eq. (2.1) one may write the interpolated action as

$$\mathcal{L}_\delta = \frac{1}{2}(\partial_0\phi)^2 - \frac{1}{2}\eta^2\phi^2 - \delta\frac{\lambda}{4}\phi^4 + \delta\frac{1}{2}\eta^2\phi^2 \; , \tag{2.4}$$

from which one obtains the perturbative order-δ result [21]

$$\mathcal{E}^{(1)} = -\frac{i}{2}\int_{-\infty}^{+\infty}\frac{dp}{2\pi}\ln[p^2-\eta^2] - \delta\frac{i}{2}\int_{-\infty}^{+\infty}\frac{dp}{2\pi}\frac{\eta^2}{p^2-\eta^2} - \delta\lambda\frac{3}{4}\left(\int_{-\infty}^{+\infty}\frac{dp}{2\pi}\frac{1}{p^2-\eta^2}\right)^2 + \mathcal{O}(\delta^2) \; . \tag{2.5}$$

Now, setting $\delta = 1$ and applying the PMS optimization procedure one gets

$$\bar{\eta} = 3i\lambda\int_{-\infty}^{+\infty}\frac{dp}{2\pi}\frac{1}{p^2-\bar{\eta}^2} \; , \tag{2.6}$$

which is a self-consistent mass gap equation. It can be easily checked that with this solution one resumms exactly the same contributions that would appear in the usual Hartree approximation. The same procedure will capture the physics which arises from exchange terms at order-δ^2 where the first contribution of this type appears together with order-δ^2 direct (Hartree) contributions. Moreover, as shown in other applications [27], the result furnished by Eq. (2.6) remains valid at second order if one considers only the direct terms and this pattern is valid at any order in δ. The actual value predicted at this lowest order is $\mathcal{E}^{(1)} = \mathcal{E}^{\rm Hartree} \sim \lambda^{1/3}0.429$ which is only about 2% greater than the exact result. As shown in Ref. [21] this result can still be improved as one goes to higher orders. Here, we shall be mainly concerned with the nonperturbative evaluation of the vacuum expectation value $\langle\phi^2\rangle$. This quantity, whose exact result is $\langle\phi^2\rangle^{\rm exact} = \lambda^{-1/3}0.456119955748\ldots$ [28], was also evaluated in Ref. [21]. The optimum values were obtained with $\bar{\eta}$ values coming from its direct optimization and also from the optimization of $\mathcal{E}$. At order-δ the value $\langle\phi^2\rangle^{(1)} = \lambda^{-1/3}0.446456$ was obtained from the direct optimization ($\bar{\eta} = 1.259921$) and $\langle\phi^2\rangle^{(1)} = \lambda^{-1/3}0.436789$ was obtained from the injection of $\bar{\eta} = 1.14471$, which was generated by the optimization of $\mathcal{E}$. One then sees that the optimum $\langle\phi^2\rangle$ numerical values generated by the two optimization procedures are very similar which could be expected since, at each order, the diagrams which contribute to $\langle\phi^2\rangle$ and $\mathcal{E}$ have the same structure.

At this stage it should be clear how nonperturbative results may be generated, through the variational PMS procedure, from the perturbative evaluation of physical quantities. As already mentioned, the effective model to be considered in the sequel for the description of the dilute Bose gas temperature bears may similarities with the AO. The main differences being the number of space-time dimensions concerning each case (which means that one has to deal with ultraviolet divergences in three dimensions) and the fact that the former is used to investigate a phase transition. Technically, as we shall see, this translates into extra difficulties due to the Hugenholtz-Pines theorem which washes out direct (tadpole) contributions, meaning that the first non-trivial contributions to $\langle\phi^2\rangle$ start at the three-loop level via two-loop self-energies. Apart from the quantum mechanical applications [21, 22, 23, 24], the LDE was successfully applied to the description of mesoscopic systems [29], nuclear matter properties [27], phase transitions in the scalar

$\lambda\phi^4$ model [30, 31] as well as in the Gross-Neveu model [32], investigation of chiral symmetry phenomena in QCD [33] and in the determination of the equation of state for the Ising model [34]. It is worth mentioning that the application of the LDE to the scalar $O(N) \times O(N)$ model [35] has allowed to investigate the nonperturbative phenomenon of symmetry nonrestoration at high temperatures further than it was possible with other standard nonperturbative methods.

The first application of this method to the present problem was performed in Ref. [4], where only the first non-trivial contribution, which appears at order-δ^2, was considered. A successful extension to the ultra-relativistic case was performed by Bedingham and Evans in Ref. [36].

B. The interpolated theory for the zero frequency Matsubara modes

One can now write the interpolated version of the effective model described by Eq. (1.10). Before doing that let us rewrite $r_{\rm bare} = r + A$ where A is a mass counterterm coefficient. This counterterm is the only one effectively needed within the modified minimal subtraction ($\overline{\rm MS}$) renormalization scheme which we will adopt here. Then, one can choose

$$S_0 = \frac{1}{2}\left[|\nabla\phi|^2 + \eta^2\phi^2\right] \ , \tag{2.7}$$

obtaining

$$S_\delta = \int d^3x \left[\frac{1}{2}|\nabla\phi|^2 + \frac{1}{2}\eta^2\phi^2 + \frac{\delta}{2}(r-\eta^2)\phi^2 + \frac{\delta u}{4!}(\phi^2)^2 + \frac{\delta}{2}A_\delta\phi^2\right] \ . \tag{2.8}$$

Note that we have treated r (r_c at the critical point) as an interaction, since this quantity has a critical value which is at least of order δ. The Feynman rules for this theory, in Euclidean space, are $-\delta r$, $\delta\eta^2$ and $-\delta A_\delta$, for the quadratic vertices and $-\delta u$ for the quartic vertex. The propagator is given by

$$G^{(0)}(p) = [p^2 + \eta^2]^{-1} \ . \tag{2.9}$$

The corresponding diagrams for these rules are shown in Fig. 1. Note that η acts naturally as an infrared cutoff so we do not have to worry about these type of divergences. By introducing only quadratic terms the LDE interpolation does not alter the polynomial structure, and hence the renormalizability, of the theory.

In general, the counterterm coefficients appearing in the interpolated theory have a trivial dependence on the bookkeeping parameter and the renormalization process can be consistently achieved with the interpolated theory exactly as in ordinary perturbation theory. Once inserted into a diagram, the extra quadratic vertex proportional to $\delta\eta^2$ brings in more propagators decreasing the ultraviolet degree of divergence. We point out that renormalization should be carried out before the optimization process to ensure that the optimum value $\bar{\eta}$ is a finite quantity. The interested reader is referred to Refs. [30, 35] for more details concerning renormalization within the LDE.

Requiring that at the critical temperature the original system must exhibit infinite correlation length, means that, at T_c and $\delta = 1$ (the original theory), the full propagator $G^{(\delta)}(p)$, given by

$$G^{(\delta)}(p) = \left[p^2 + \eta^2 + \delta r - \delta\eta^2 + \Sigma^{(\delta)}_{\rm ren}(p)\right]^{-1} \ , \tag{2.10}$$

must satisfy $G^{(\delta)}(0)^{-1} = 0$, which implies

$$\delta r_c^{(\delta)} = -\Sigma^{(\delta)}_{\rm ren}(0) \ . \tag{2.11}$$

The above equation is equivalent to the Hugenholtz-Pines theorem applied to the LDE. The relation Eq. (2.11) shows that, to order-δ^n, the quantity $\delta r_c^{(n)}$ is directly obtained from the evaluation of $\Sigma^{(n)}_{\rm ren}(0)$. As discussed in the introduction, we will use the Feynman rules described above to evaluate perturbatively the self-energy $\Sigma^{(\delta)}_{\rm ren}(p)$ to order-δ^4 from which we will get the nonperturbative values for κ and $\mathcal{R}$ by using the PMS optimization procedure. The subscript "ren" in the self-energy means that this quantity also contains all diagrams which arise from the mass

counterterm vertex proportional to δA_δ. For our purposes, the easiest way to obtain a perturbative expansion for $\langle\phi^2\rangle_u$ is to start from

$$\langle\phi^2\rangle_u^{(\delta)} = \sum_{i=1}^{N}\langle\phi_i^2\rangle_u^{(\delta)} = N\int\frac{d^3p}{(2\pi)^3}G^{(\delta)}(p) = \int\frac{d^3p}{(2\pi)^3}\frac{N}{p^2+\eta^2}\left[1+\frac{\delta(r_c^{(\delta)}-\eta^2)+\Sigma_{\rm ren}^{(\delta)}(p)}{p^2+\eta^2}\right]^{-1} . \tag{2.12}$$

Like $\delta r_c^{(n)}$, the order-δ^n quantity $\langle\phi^2\rangle_u^{(\delta)}$ is obtained by evaluating the self-energies to that order and subsequently expanding the series on the RHS of Eq. (2.12). Therefore, to obtain $\mathcal{R}$ and κ to order-δ^4 we need to consider the fifty four self-energy contributions shown in Fig. 1.

III. EVALUATION OF r_c TO $\mathcal{O}(\delta^4)$

According to the Hugenholtz-Pines theorem, $\delta r_c^{(4)}$ is obtained from the evaluation of all diagrams shown in Fig. 1 with zero external momentum. To make this paper more pedagogical, let us do a step by step evaluation of r_c up to order-δ^2. To order-δ one has only the tadpole contribution, a direct application of the Feynman rules for the interpolated theory and dimensional regularization (see appendix for more details) gives the finite contribution

$$-\delta r_c^{(1)} = \Sigma_{\rm ren}^{(1)}(0) = -\delta u\frac{\eta}{8\pi}\left(\frac{N+2}{3}\right) . \tag{3.1}$$

Carrying on to order δ^2 one considers the contributions depicted by the first five diagrams of Fig. 1, which give

$$\begin{aligned} -\delta r_c^{(2)} \;&=\; \Sigma_{\rm ren}^{(2)}(0) = -\delta u\frac{\eta}{8\pi}\left(\frac{N+2}{3}\right) + \delta^2 u\frac{\eta}{16\pi}\left(\frac{N+2}{3}\right) - \delta^2\frac{u}{16\pi}\frac{r_c}{\eta}\left(\frac{N+2}{3}\right) \\ &+\; \delta^2\frac{u^2}{128\pi}\left(\frac{N+2}{3}\right)^2 - \delta^2\frac{u^2}{(8\pi)^2}\frac{(N+2)}{18}\left[\frac{1}{\epsilon}+4\ln\left(\frac{M}{\eta}\right)-2.394\right] + \delta A_\delta + \mathcal{O}(\delta^3) , \end{aligned} \tag{3.2}$$

where M is an arbitrary $\overline{\rm MS}$ mass scale[2]. Now, one replaces δr_c which appears at the right hand side with the value $\delta r_c^{(1)}$ obtained at the previous order so that the right hand side *remains* of order δ^2. Next, one sees that the setting sun, whose explicit evaluation follows those performed in the appendix [see Eq.(A18)], displays an ultraviolet pole as $\epsilon\to\infty$. In fact, within dimensional regularization, the only primitive ultraviolet divergence associated with the effective super-renormalizable three dimensional theory steams from the setting sun type of diagram with three internal propagators. The pole associated with this divergence fixes the mass counterterm coefficient in the modified minimal subtraction renormalization scheme,

$$\delta A_\delta = \delta^2\frac{u^2}{(8\pi)^2}\frac{(N+2)}{18}\frac{1}{\epsilon} . \tag{3.3}$$

As usual, this "vertex" must be considered also at higher orders (see Fig. 1) so diagrams whose divergences arise from "setting sun" sub-diagrams may be rendered finite [20]. Now, it is easy to see how the "double scoop" contribution (fourth term on the RHS of Eq. (3.2)) is exactly canceled due to the HP condition applied to r_c at first order. One then gets the finite second order result

$$-\delta r_c^{(2)} = \Sigma_{\rm ren}^{(2)}(0) = -\delta u\frac{\eta}{8\pi}\left(\frac{N+2}{3}\right) + \delta^2 u\frac{\eta}{16\pi}\left(\frac{N+2}{3}\right) - \delta^2\frac{u^2}{(8\pi)^2}\frac{(N+2)}{18}\left[4\ln\left(\frac{M}{\eta}\right)-2.394\right] + \mathcal{O}(\delta^3) \tag{3.4}$$

Also at higher orders many contributions cancel. In special, any diagram with one or more tadpole sub-diagram(s), like the "double scoop" discussed at order-δ^2, disappear. Then, the diagrams which really contribute to $\delta r_c^{(4)}$ are

[2] Note that our choice for the integral measure, Eq. (A1), has already taken care of constants like 4π and e^{γ_E} which, otherwise, would appear in the setting sun logarithmic term.

those shown in Fig. 2, where one must consider the external lines as carrying zero momentum. At the same time, counterterm diagrams associated with the zero external momentum setting sun diagram (or sub-diagrams) could have been suppressed from that figure. However, we prefer to write them explicitly so that the same figure can be used again, facilitating the discussion in the next section. Using the results obtained in the appendix one obtains the fourth order result

$$
\begin{aligned}
-\delta r_c^{(4)} &= \Sigma_{\rm ren}^{(4)}(0) = -\delta u \frac{\eta}{8\pi}\left(\frac{N+2}{3}\right) + \delta^2 u \frac{\eta}{16\pi}\left(\frac{N+2}{3}\right) - \delta^2 \frac{u^2}{(4\pi)^2}\frac{(N+2)}{18}\left[\ln\left(\frac{M}{\eta}\right) - 0.59775\right] \\
&+ \delta^3 u \frac{\eta}{64\pi}\left(\frac{N+2}{3}\right) - \delta^3 \frac{u^3}{\eta}\frac{(N+2)^2}{108(4\pi)^3}[0.143848] + \delta^3 \frac{u^3}{\eta}\frac{\left(16+10N+N^2\right)}{(4\pi)^5 108}[81.076] \\
&- \delta^3 u^2 \frac{(N+2)}{18(4\pi)^2}[0.498] + \delta^4 u \frac{\eta}{128\pi}\left(\frac{N+2}{3}\right) - \delta^4 \frac{u^3}{\eta}\frac{(N+2)^2}{108(4\pi)^3}[0.0610] \\
&+ \delta^4 \frac{u^4}{\eta^2}\frac{(N+2)}{6(4\pi)^6}\frac{\left(16+10N+N^2\right)}{108}[8.09927] - \delta^4 \frac{u^3}{\eta}\frac{(N+2)^2}{108(4\pi)^3}[0.011788] - \delta^4 u^2 \frac{(N+2)}{18(4\pi)^2}[0.166492] \\
&- \delta^4 u^2 \frac{(N+2)}{18(4\pi)^2}[0.0834] + \delta^4 \frac{u^3}{\eta}\frac{\left(16+10N+N^2\right)}{(4\pi)^5 108}[10.240] + \delta^4 \frac{u^3}{\eta}\frac{\left(16+10N+N^2\right)}{(4\pi)^5 108}[30.31096] \\
&- \delta^4 \frac{u^4}{\eta^2}\frac{\left(40+32N+8N^2+N^3\right)}{(4\pi)^6 648}[20.43048] - \delta^4 \frac{u^4}{\eta^2}\frac{\left(44+32N+5N^2\right)}{(4\pi)^6 324}[12.04114] \\
&- \delta^4 \frac{u^4}{\eta^2}\frac{\left(44+32N+5N^2\right)}{(4\pi)^6 324}[17.00434] + \delta^4 \frac{u^4}{\eta^2}\frac{(N+2)^2}{(18)^2(4\pi)^6}[2.8726] + \mathcal{O}(\delta^5)\ . \qquad (3.5)
\end{aligned}
$$

The scale dependence of this quantity will be discussed in Section V.

IV. EVALUATION OF $\langle\phi^2\rangle_u$ TO ORDER δ^4

In principle, to obtain $\langle\phi^2\rangle_u^{(4)}$ one should consider all contributions to the self-energy $\Sigma_{\rm ren}^{(4)}(p)$ given by the diagrams of Fig. 1 with external momentum p. However, thanks to results of the previous section, one does not have to do the evaluation of all those graphs explicitly at this stage. In fact, one can immediately reduce the number of graphs to be considered by substituting the vertex δr with the the appropriate critical value δr_c obtained in the previous section. Then, as for $\Sigma_{\rm ren}^{(4)}(0)$, the set of diagrams which effectively contribute to $\Sigma_{\rm ren}^{(4)}(p)$ reduces to those shown in Fig. 2, but now one must consider the external lines as carrying momentum p. Substituting Eq. (3.5) into Eq. (2.12) one sees that the quantity which matters for the evaluation of $\langle\phi^2\rangle_u^{(4)}$ is $\Sigma_{\rm ren}^{(4)}(p) - \Sigma_{\rm ren}^{(4)}(0)$. Diagramatically, this quantity is given by taking the graphs of Fig. 2 with zero external momentum and subtracting them from the same diagrams with external momentum p. This means that all diagrams which do not depend on the external momentum will not contribute in the evaluation of $\langle\phi^2\rangle$ at the critical point. For example, all the tadpole diagrams with any type of sub-diagrams will not contribute. As expected, the mass counterterm is a redundant quantity in the evaluation of $\langle\phi^2\rangle_u^{(n)}$ because this quantity depends on the difference

$$
\Sigma_{\rm ren}^{(n)}(p) - \Sigma_{\rm ren}^{(n)}(0) = [\Sigma_{\rm div}^{(n)}(p) + \Sigma_{\rm ct}^{(n)}(p)] - [\Sigma_{\rm div}^{(n)}(0) + \Sigma_{\rm ct}^{(n)}(0)]\ , \qquad (4.1)
$$

where $\Sigma_{\rm div}^{(n)}(p)$ is the divergent self-energy. For a general renormalizable theory, the quantity $\Sigma_{\rm ct}^{(n)}(p)$ represents all counterterms associated with the parameters of the theory (such as masses and coupling constants) as well as the wave-function counterterm associated with any eventual momentum dependent pole. At the same time, $\Sigma_{\rm ct}^{(n)}(0)$ involves the same counterterms except for the wave-function one. However, as we have already emphasized, in the three-dimensional case the only type of primitive divergence requires only a mass counterterm, which is the same for $\Sigma_{\rm div}^{(n)}(p)$ and $\Sigma_{\rm div}^{(n)}(0)$. This means that in our case, $\Sigma_{\rm div}^{(n)}(p) - \Sigma_{\rm div}^{(n)}(0)$ is always a finite quantity as shown explicitly in the appendix where it is also shown that this quantity is scale independent, as opposed to r_c. Therefore, the type of diagrams which really matter for the evaluation of $\langle\phi^2\rangle_u^{(4)}$ are those shown in Fig. 3, which can be obtained expanding Eq. (2.12) to $\mathcal{O}(\delta^4)$. Following the sequence of diagrams shown in Fig. 3 one can write

$$
\langle\phi^2\rangle_u = \int \frac{d^3p}{(2\pi)^3}\frac{N}{p^2+\eta^2}\left\{1 + \frac{\delta\eta^2}{p^2+\eta^2} + \frac{\delta^2\eta^4}{(p^2+\eta^2)^2} + \frac{\delta^3\eta^6}{(p^2+\eta^2)^3} + \frac{\delta^4\eta^8}{(p^2+\eta^2)^4}\right.
$$

$$
\begin{aligned}
&- \delta^2\frac{[\Sigma_1(p)-\Sigma_1(0)]}{p^2+\eta^2} - \delta^3\frac{2\eta^2[\Sigma_1(p)-\Sigma_1(0)]}{(p^2+\eta^2)^2} - \delta^3\frac{[\Sigma_2(p)-\Sigma_2(0)]}{p^2+\eta^2}\\
&- \delta^3\frac{[\Sigma_3(p)-\Sigma_3(0)]}{p^2+\eta^2} - \delta^4\frac{3\eta^4[\Sigma_1(p)-\Sigma_1(0)]}{(p^2+\eta^2)^3} - \delta^4\frac{2\eta^2[\Sigma_2(p)-\Sigma_2(0)]}{(p^2+\eta^2)^2}\\
&- \delta^4\frac{[\Sigma_4(p)-\Sigma_4(0)]}{(p^2+\eta^2)} - \delta^4\frac{[\Sigma_7(p)-\Sigma_7(0)]}{(p^2+\eta^2)} - \delta^4\frac{2\eta^2[\Sigma_3(p)-\Sigma_3(0)]}{(p^2+\eta^2)^2}\\
&- \delta^4\frac{[\Sigma_{10}(p)-\Sigma_{10}(0)]}{(p^2+\eta^2)} - \delta^4\frac{[\Sigma_5(p)-\Sigma_5(0)]}{(p^2+\eta^2)} + \delta^4\frac{[\Sigma_1(p)-\Sigma_1(0)]^2}{(p^2+\eta^2)^2}\\
&- \delta^4\frac{[\Sigma_6(p)-\Sigma_6(0)]}{(p^2+\eta^2)} - \delta^4\frac{[\Sigma_8(p)-\Sigma_8(0)]}{(p^2+\eta^2)} - \delta^4\frac{[\Sigma_9(p)-\Sigma_9(0)]}{(p^2+\eta^2)}\\
&- \delta^4\frac{[\Sigma_{11}(p)-\Sigma_{11}(0)]}{(p^2+\eta^2)} + \mathcal{O}(\delta^5)\Big\} \ . \qquad (4.2)
\end{aligned}
$$

The details of the explicit evaluation of the Σ_i terms are given in the appendix. The final result we obtain is

$$
\begin{aligned}
\langle\phi^2\rangle_u \ &= \ -\frac{N\eta}{4\pi} + \frac{\delta}{2}\frac{N\eta}{4\pi} + \frac{\delta^2}{8}\frac{N\eta}{4\pi} + \frac{\delta^3}{16}\frac{N\eta}{4\pi} + \frac{\delta^4}{128}\frac{5N\eta}{4\pi}\\
&- \delta^2\frac{u^2}{\eta}\frac{N(N+2)}{18(4\pi)^3}[0.143848] - \delta^3\frac{u^2}{\eta}\frac{N(N+2)}{18(4\pi)^3}[0.01168] - \delta^3\frac{u^2}{\eta}\frac{N(N+2)}{18(4\pi)^3}[0.0610]\\
&+ \delta^3\frac{u^3}{\eta^2}\frac{N}{(4\pi)^6}\frac{\left(16+10N+N^2\right)}{108}[8.09927] - \delta^4\frac{u^2}{\eta}\frac{N(N+2)}{18(4\pi)^3}[2.8270\times10^{-3}]\\
&- \delta^4\frac{u^2}{\eta}\frac{N(N+2)}{18(4\pi)^3}[7.7318\times10^{-3}] - \delta^4\frac{u^2}{\eta}\frac{N(N+2)}{18(4\pi)^3}[0.02461] - \delta^4\frac{u^2}{\eta}\frac{N(N+2)}{18(4\pi)^3}[0.01825]\\
&+ \delta^4\frac{u^3}{\eta^2}\frac{N}{(4\pi)^6}\frac{\left(16+10N+N^2\right)}{108}[0.85984] + \delta^4\frac{u^3}{\eta^2}\frac{N}{(4\pi)^6}\frac{\left(16+10N+N^2\right)}{108}[1.937786]\\
&+ \delta^4\frac{u^3}{\eta^2}\frac{N}{(4\pi)^6}\frac{\left(16+10N+N^2\right)}{108}[5.30476] - \delta^4\frac{u^4}{\eta^3}\frac{N(N+2)^2}{(18)^2(4\pi)^7}[0.87339]\\
&- \delta^4\frac{u^4}{\eta^3}\frac{N}{(4\pi)^7}\frac{\left(40+32N+8N^2+N^3\right)}{648}[3.15904767] - \delta^4\frac{u^4}{\eta^3}\frac{N}{(4\pi)^7}\frac{\left(44+32N+5N^2\right)}{324}[1.70959]\\
&- \delta^4\frac{u^4}{\eta^3}\frac{N(N+2)^2}{(18)^2(4\pi)^7}[4.4411] - \delta^4\frac{u^4}{\eta^3}\frac{N}{(4\pi)^7}\frac{\left(44+32N+5N^2\right)}{324}[2.37741] + \mathcal{O}(\delta^5) \ . \qquad (4.3)
\end{aligned}
$$

V. NUMERICAL RESULTS FOR THE TEMPERATURE SHIFT

In this section we will turn our, so far, perturbative evaluation into nonperturbative results using the PMS optimization prescription. Our analysis of results, including the selection of the relevant optima, will follow closely those adopted in the applications which proved the convergence of this method for the anharmonic oscillator [21, 22, 23, 24]. Some of the guidelines developed on those studies are essential for our present application. Let us start the optimization process with the scale independent quantity $\langle\phi^2\rangle_u^{(\delta)}$ whose recent Monte Carlo estimate is $\langle\phi^2\rangle_u = -0.001198(17)\,u$ [8]. Before optimizing let us remark that all contributions to $\langle\phi^2\rangle_u^{(n)}$ are proportional to $\delta^n u^n \eta^{1-n}$ and therefore, the PMS condition will imply solving a polynomial equation of degree n. As one may expect, many of those n roots which determine the optimum $\bar{\eta}$ will be complex. Also, as observed in the anharmonic oscillator studies, most of the time the best results are in fact generated by the complex solutions [21]. Since η is arbitrary we have no justification, a priori, to throw away its complex part. This means that our optimized physical quantities $\langle\phi^2\rangle_u$ and r_c will have, eventually, complex parts whose meaning is to be interpreted according to the physics. Here, these two quantities are ultimately used to determine a strictly real physical quantity defined by the critical temperature. Therefore, for our purposes the complex parts of those two physical quantities are not relevant and will not be considered. Note that the imaginary parts of optimized physical observables have also been dropped in Ref. [21] where a different, but still valid, physical argument has been used. Finally, we shall follow the original PMS prescription [18] and optimize $\langle\phi^2\rangle_u^{(\delta)}$ and $r_c^{(\delta)}$ separately. This procedure was also adopted in the ultra relativistic case where it has produced good results [36].

By truncating Eq. (4.3) to the first nontrivial order, order-δ^2, setting $\delta = 1$ and by applying the PMS, one gets the two real roots

$$\bar{\eta} = \pm 0.0232332\, u \ , \tag{5.1}$$

which give

$$\langle \phi^2 \rangle_u^{(2)} = \mp 0.002777326\, u \ . \tag{5.2}$$

Applying the PMS to $\langle \phi^2 \rangle_u^{(\delta)}$ at order-δ^3 one obtains the following three solutions. The first, $\bar{\eta} = -0.0475422\, u$ gives $\langle \phi^2 \rangle_u^{(3)} = 0.0045505\, u$ while the other two

$$\bar{\eta} = (0.0237711 \pm 0.0268995 i)\, u \ , \tag{5.3}$$

yield

$$\langle \phi^2 \rangle_u^{(3)} = -(0.00221912 \pm 0.00150245 i)\, u \ . \tag{5.4}$$

At order-δ^4 one obtains the real solutions $\bar{\eta} = 0.0439352\, u$ which gives $\langle \phi^2 \rangle_u^{(4)} = -0.00293974\ u$ and $\bar{\eta} = -0.0697993\, u$ which gives $\langle \phi^2 \rangle_u^{(4)} = 0.00483554\, u$. The complex solutions are

$$\bar{\eta} = (0.0129321 \pm 0.04676942 i)\, u \ , \tag{5.5}$$

from which one gets

$$\langle \phi^2 \rangle_u^{(4)} = -(0.00134323 \pm 0.00213104 i)\, u \ . \tag{5.6}$$

In order to select the appropriate roots we recur again to the AO convergence studies where the existence and behavior of optima families was fully investigated to order-δ^{47} [21]. There, it was observed that at a given order n each PMS solution belongs to a different family, the exception being complex conjugate solutions which belong to the same family. It was observed that, in the complex plane, the first member of a new family always lies on the real axis and also that a new family arises as n is increased by 2. Supposing that these findings may also be used in our three-dimensional problem, we may identify two families whose first members lie on the real axis at order-δ^2. Family 1 starts with the positive real solution $\bar{\eta} = 0.0232332\, u$ and family 2 with the negative real solution $\bar{\eta} = -0.0232332\, u$. No new families arise when one goes to the next order and the real negative solution $\bar{\eta} = -0.0475422\, u$ is just another member of the family of negative real solutions (2) while the complex conjugate optima with positive real parts $\bar{\eta} = (0.0237711 \pm 0.0268995 i)\, u$ are taken as belonging to family 1. At order-δ^4, family 2 gets another member given by $\bar{\eta} = -0.06983\, u$, whereas family 1 gets $\bar{\eta} = (0.0129321 \pm 0.04676942 i)\, u$.

As we have increased the order by 2 one effectively sees the appearance of a new family whose first member lies on the real axis and is given by $\bar{\eta} = 0.0439352\, u$. We can now roughly examine the convergence of our results. The values obtained with the optima belonging to family 1 are $\langle \phi^2 \rangle_u^{(2)} = -0.002777326\ u$, $\mathrm{Re}[\langle \phi^2 \rangle_u^{(3)}] = -0.00221912 u$ and $\mathrm{Re}[\langle \phi^2 \rangle_u^{(4)}] = -0.00134323\ u$. Family 2 gives $\langle \phi^2 \rangle_u^{(2)} = 0.002777326\ u$, $\langle \phi^2 \rangle_u^{(3)} = 0.00405505\ u$ and $\langle \phi^2 \rangle_u^{(4)} = 0.00483554\ u$, whereas family 3 gives $\langle \phi^2 \rangle_u^{(4)} = -0.00293974\ u$. Note that the first $\langle \phi^2 \rangle_u$ value predicted by family 3 is only about 5% greater than the first value predicted by family 1. It is very likely that family 3 will become complex and, as for the AO, as we go to higher orders families 1 and 3 will predict very similar values converging to the exact value. Family 2, on the other hand, seems to have only real components. It predicts values of $\langle \phi^2 \rangle_u$ which increase order by order with a sign which is opposite to the one predicted by families 1 and 3. Moreover, in the AO, it was observed that the complex families have better convergence behavior than the purely real families. This analogy indicates that family 1 should produce converging results.

We can justify pushing the analogy in between our effective three dimensional model and its one dimensional version that far by remarking that, at least to the order we consider here, $\langle \phi^2 \rangle_u^{(\delta)}$ can be expressed as a power expansion of the form

$$\langle\phi^2\rangle_u^{(4)} = N\sum_{i=0}^{4}(-1)^{i+1}(u\delta)^i[\eta(1-\delta)^{1/2}]^{1-i}B_i\,, \tag{5.7}$$

where $B_0 \sim 10^{-1}$, $B_1 = 0$, $B_2 \sim 10^{-5}$, $B_3 \sim 10^{-6}$ and $B_4 \sim 10^{-7}$. This structure is similar to the one found in the one dimensional case. This hints that both models may have similar convergence properties making our procedure more legitimate. It is also worth pointing out that in our previous work, Ref. [4], we had only the order-δ^2 result and it was not possible to do the same type of comparison among the solutions to find an acceptable pattern of order by order corrections. There, to choose among the two possible solutions, $\langle\phi^2\rangle_u^{(2)} = \mp 0.002777326\, u$, we had to use different arguments and were also guided by results found with other methods. By considering higher orders, as we have done here, we can overcome this problem and the negative result, $\langle\phi^2\rangle_u^{(2)} = -0.002777326\, u$, naturally appears as the one which belongs to the most well behaved sequence of order by order corrections.

We are now in position to evaluate $u\kappa = \Delta\langle\phi^2\rangle_c^{(\delta)}$, so that c_1 can be determined via Eq. (1.7) with the optima contained in family 1. As one could expect, $\bar{\eta}$ is always proportional to u since the latter quantity is the only quantity with mass dimensions appearing in $\langle\phi^2\rangle_u^{(\delta)}$. This means that the optimum value for the non-interacting vacuum expectation value $\langle\phi^2\rangle_0^{(\delta)}$ will be zero at any order. This agrees with the results of Ref. [8], where it was shown that this is indeed the value obtained when the theory is regularized with dimensional regularization. Then, $u\kappa = \Delta\langle\phi^2\rangle_c^{(n)} = \langle\phi^2\rangle_u^{(n)}$ from which one finally obtains $c_1 = 3.06$, $c_1 = 2.45$ and $c_1 = 1.48$ at order δ^2, δ^3 and δ^4, respectively[3]. These results are compared with other analytical and numerical results in Table 1.

It is instructive to examine the topology of the diagrams contributing at each order so that we can establish the links with other nonperturbative methods. At second order the non-trivial contribution arises from the setting sun (one plain bubble) type of diagram. At third order one has, besides the setting suns with insertions, a new contribution which arises from the two plain bubble type of diagram (ninth graph shown in Fig. 3). However, this contribution, belongs with the setting sun to a class of diagrams that would appear in a plain bubble sum or in the leading order of a $1/N$ type of calculation. At fourth order one considers again a three plain bubble contribution (eighteenth diagram of Fig. 3) but more radical changes arise via other type of vertex corrections like the correction to the plain bubble that comes from the nineteenth and twentieth diagrams of Fig. 3. Finally, the last diagram contains a different type of vertex correction that would appear on a ladder type of summation. In fact, one can easily evaluate which are the individual contributions of the five-loop diagrams shown in Fig. 3. The first of them gives a contribution (in unities of u^4/η^3) of approximately 1.9×10^{-9}, the second gives 2.8×10^{-8}, the third 2.7×10^{-8}, the fourth 8.86×10^{-9} and the fifth gives 2.6×10^{-8}. These numbers show that, at this order, the total contribution from the ladder and bubble correction type of contributions (third and fifth) are effectively twice that of the plain three bubble one.

It is also easy to see by drawing that the only corrections which may appear at odd orders are those due to the *doubling* of a bubble that already appeared at the previous order (increasing the "bubble chain"). At the same time, at even orders, one is allowed to *insert* a new bubble anywhere creating diagrams with completely different topologies. In other words, in a perturbative expansion of $\langle\phi^2\rangle_u^{(\delta)}$, new topological classes of graphs can arise only at even orders.

One can now appreciate that the reason our order-δ^2 result $c_1 = 3.06$ [4], obtained by optimizing only one setting sun contribution, compares so well with the value $c_1 = 2.90$, found by resumming setting sun contributions in a self-consistent way [1], is a consequence that both approximations consider the same type of diagrams. On the other hand, when going to order-δ^3 one considers a new diagram but which, together with the setting sun, would also be considered in a large-N calculation. In the LED, its effect is to reduce the second order result to $c_1 = 2.45$. Let us consider, for the moment, the only order-δ^4 contribution that would also be considered in a large-N calculation. Graphically this contribution is displayed by the second of the five-loop terms in Fig. 3. Not surprisingly, we obtain the value $c_1 = 2.32$ which is very close to the $c_1 = 2.33$ value obtained with the $1/N$ method at leading order [2] and the numerical differences may be due to the fact that we have considered our symmetry factors in full, not only the highest power of N. The four remaining five-loop contributions would be considered in an $1/N$ type of calculation to the next order. Such a calculation has been performed by Arnold and Tomásik [3] who found $c_1 = 1.71$, which is approximately 27% smaller than the leading order result. In our case this fact is confirmed at order-δ^4, where the net effect of considering diagrams which would belong to a next to leading order $1/N$ evaluation is to decrease the value $c_1 = 2.32$ obtained with the graph that would appear at leading order in the same approximation by roughly 35%. As before the numerical differences must be due to the full consideration of powers of N in each symmetry factor. It is

[3] At this stage it should be clear that it is preferable to optimize $\langle\phi^2\rangle_u^{(\delta)}$ rather than $\Delta\langle\phi^2\rangle^{(\delta)}$ because the latter quantity is less η dependent.

not our aim to establish here a formal relationship among the different approximations. Nevertheless, the discussion above can serve as a guide to understand how the LDE captures part of the nonperturbative physics contained within the SCR and $1/N$ approximations.

In order to evaluate the coefficient c_2'' we now turn to the optimization of the scale dependent r_c. Setting $\delta = 1$ and applying the PMS to $r_c^{(2)}$ generates one positive, real optimum given by $\bar{\eta} = u/6\pi$. It is important to note that this PMS solution is a scale independent quantity. In fact, r_c depends on the ($\overline{\rm MS}$) mass scale through the term proportional to $u^2 \ln(M/\eta)$ which appears in the order-δ^2 setting sun term. It is then easy to see that when this term is derived with respect to η the scale dependence automatically disappears turning our optimization procedure into a scale independent process. As discussed below this situation will be verified at any order in δ.

Next, in order to get a numerical result for the optimized r_c one must fix a scale and here we choose $M = u/3$ which is the same scale [4] used by Arnold, Moore and Tomásik in Ref. [8] where the result found for this quantity is $r_c(M = u/3) = 0.001920(2)\, u^2$. The relation in between the values of $r_c^{(\delta)}$, evaluated at two different ($\overline{\rm MS}$) mass scales M_1 and M_2, can be obtained from Eq. (3.5) and reads

$$\frac{r_c^{(4)}(M_1)}{u^2} = \frac{r_c^{(4)}(M_2)}{u^2} + \frac{(N+2)}{18(4\pi)^2} \ln\left(\frac{M_1}{M_2}\right) \; . \tag{5.8}$$

It is not too difficult to see that this relation will be verified at any order in δ. At order-δ^2 the only diagram which is scale dependent is the setting sun. At a higher order ($n \geq 3$) this order-δ^2 contribution can only appear as a subdiagram. At the same order a similar graph appears, but this time δr replaces the setting sun insertion. However, the "vertex" δr_c is always replaced (see Sec. III) by its expansion in δ which contains, at order-δ^2, exactly the same scale dependent term as given by the setting sun, with a reversed sign. This means that, apart from the order-δ^2 setting sun, all contributions to $\delta r_c^{(n)}$ are automatically scale independent. Optimizing our order-δ^2 result one gets

$$r_c^{(2)} = 0.00315236\, u^2 \; . \tag{5.9}$$

Proceeding to next order the PMS gives two complex solutions, $\bar{\eta} = (0.0353678 \pm 0.0550091 i)u^2$ which yield

$$r_c^{(3)} = (0.00221321 \pm 0.00009661 i)\, u^2 \; . \tag{5.10}$$

Finally, the order-δ^4 optimization results are the real solution $\bar{\eta} = 0.0659334\, u$, which yields $r_c^{(4)} = 0.00246153\, u^2$ and the complex solutions $\bar{\eta} = (0.00947463 \pm 0.0797262 i)u^2$, which generates

$$r_c^{(4)} = (0.00165411 \pm 0.000772567 i)\, u^2 \; . \tag{5.11}$$

As in the previous case one sees that the first optima family starts with a real value at order-δ^2 and turns into a complex family at order-δ^3. At order-δ^4 it receives a new complex member. The first family generates the real values $r_c^{(2)} = 0.00315236\, u^2$, ${\rm Re}[r_c^{(3)}] = 0.00221321\, u^2$ and ${\rm Re}[r_c^{(4)}] = 0.00165411\, u^2$ which are our selected values. Then, using Eq (1.8) together with the optima values obtained for κ and $\mathcal{R}$ we obtain, order after order, the results $c_2'' = 101.4$, $c_2'' = 98.2$ and $c_2'' = 82.9$ for the order-a^2 nonperturbative coefficient. As for c_1, these results compare well with the Monte Carlo estimate, $c_2'' = 75.7 \pm 0.4$.

VI. CONCLUSIONS

We have used the linear δ expansion to evaluate nonperturbatively the numerical coefficients appearing in the expansion for the transition temperature for a dilute, homogeneous, three-dimensional Bose gas given by $T_c = T_0\{1 + c_1 a n^{1/3} + [c_2' \ln(a n^{1/3}) + c_2'']a^2 n^{2/3} + \mathcal{O}(a^3 n)\}$, where T_0 is the result for an ideal gas, a is the s-wave scattering length and n is the number density. This expansion for T_c incorporates the effects of non-zero Matsubara modes [8, 9]. While the coefficient c_2' has been exactly evaluated using perturbation theory the question about the numerical values of the

[4] Our notation for the mass scale (M) is different from the one used by the authors in Ref. [8] ($\overline{M}$).

other two coefficients, c_1 and c_2'' remains open and has been the object of recent investigations. The reason behind this difficulty is the fact that these coefficients can only be obtained in a nonperturbative way.

Due to the Hugenholtz-Pines theorem the first non-trivial contribution appears at an order where one has to consider, at least, momentum dependent two-loop self-energy diagrams. Considering higher order terms, so as to get more accurate results, becomes rapidly difficult within the existing nonperturbative methods as discussed in Ref. [9], where the authors state that the complexity of the mathematical problem does not allow a definitive prediction of the prefactor c_1, of the term linear in a, from an analytic analysis. On the other hand, two recent numerical results obtained with lattice simulations, which predict $c_1 \sim 1.30$ [5, 6, 8], are being taken very seriously. In a previous work, Ref. [4], we have applied the LDE to this problem obtaining the value $c_1 \sim 3.06$ at the first non-trivial order (δ^2). However, the quality of that application was difficult to infer, from a quantitative point of view, since only one approximant had been used. On the hand, the fact that at order-δ^2 with only one graph the optimization procedure was able to generate a result numerically similar to the one obtained with a self-consistent resummation (SCR) of two-loop momentum dependent contributions [1] was encouraging. At that time, we were not in position to elaborate any further about the convergence behavior of that result.

In the present work, we have again explicitly shown that the LDE method offers, as its major advantage, the possibility to select, evaluate and renormalize a physical quantity exactly as in the familiar perturbative framework. Here, the contributions appearing at each order are not selected according to their topology as within most nonperturbative analytical cases. Contrary to some previous unfounded criticisms, no uncontrolled errors arise in this type of perturbative calculation, most notably in this application, where even the most cumbersome five-loop contributions have been fully considered and evaluated without recurring to any approximations as shown in the appendix. Another advantage is that one does not have to worry about infrared divergences, since, during the formal evaluation of graphs, the LDE arbitrary parameter naturally acts as such before disappearing during the optimization process. Also, the fact that a convergence proof for the quantum mechanical analogue of the model considered here does exist [21, 22, 23, 24] is an extra bonus.

At first one could think that the multiplicity of possible real and complex results generated by the PMS constitutes the most serious disadvantage of the LDE. Nevertheless, the quantum mechanical convergence studies of Ref. [21], have shown how meaningful nonperturbative physical results can still be obtained. As discussed in the text, those studies have been crucial to our application for some important reasons like showing how the possible solutions gather into real and complex families and emphasizing that better results are generated by the complex ones. We recall that, although different physical arguments have been used in each case, the imaginary parts of the optimized physical observables generated by the complex families have also been dropped out in Ref. [21]. As already mentioned, our effective model displays the same series structure for the physical observable $\langle\phi^2\rangle_u^{(4)}$ as its quantum mechanical counterpart. Taking all these facts into account we were able to obtain the results $c_1 = 3.06$, $c_1 = 2.47$ and $c_1 = 1.48$ at second, third and fourth orders, respectively. Our results approach, order after order, the recent Monte Carlo estimate, $c_1 \sim 1.3$.

Comparing our results and the topology of the diagrams considered here with those belonging to the self-consistent resummation of setting suns (SCR) and the $1/N$ approximation at leading ($1/N$-LO) and next to leading ($1/N$-NLO) orders we made clear that our results are not a mere coincidence. In fact, the PMS is successively chopping, order after order, nonperturbative information contained in those approximations. Our results confirm the decrease in the value of c_1 observed successively with the SCR, $1/N$-LO and $1/N$-NLO. The numerical differences may be due to the fact that we do not make any distinction among the different powers of N which appear on the symmetry factors since the LDE was envisaged to cope with arbitrary N.

We remark that a problem regarding the sign of the coefficient c_1, which appeared in our previous application, has disappeared at this higher order evaluation. We have also investigated the quantity r_c by evaluating all self-energy contributions, with zero external momentum, up to order-δ^4. Once this quantity was optimized we have obtained the values $c_2'' = 101.4$, $c_2'' = 98.2$ and $c_2'' = 82.9$ for the next nonperturbative coefficient at second, third and fourth orders, respectively. These results are in good numerical agreement with the Monte Carlo result, $c_2'' = 75.7$ [8].

In summary our analytical investigation seems to support, order by order, the results obtained with other three analytical nonperturbative methods. Our fourth-order numerical results compare well with the recent results found in Refs. [5, 6, 8]. Additionally, there is an exciting possibility that the method may offer a way of making a definitive analytical prediction for the nonperturbative coefficients c_1 and c_2'', which we are currently investigating.

Acknowledgments

The authors would like to thank Hagen Kleinert and Axel Pelster for their help concerning the general N symmetry factors and Philippe Garcia for discussing the selection of the optima. F.F.S.C., M.B.P. and R.O.R. were partially supported by Conselho Nacional de Desenvolvimento Científico e Tecnológico (CNPq-Brazil). R.O.R. also thanks

partial support from the "Mr. Tompkins Fund for Cosmology and Field Theory" at Dartmouth. P.S. was partially supported by Associação Catarinense das Fundações Educacionais (ACAFE-Brazil).

APPENDIX A: EVALUATING THE HIGHER LOOP TERMS

To make this work self-contained we shall outline, in this appendix, the details of the explicit evaluation of all Feynman diagrams considered in the evaluation of $\langle\phi^2\rangle_u^{(4)}$ for arbitrary N. We also remark that working out symmetry factors for many loop contributions with generic N is a problem on its own. Here, we have used the methods developed by Kleinert's group in Berlin [37].

We regularize all diagrams with dimensional regularization in arbitrary dimensions $d = 3 - 2\epsilon$ and carry the renormalization with the modified minimal subtraction scheme ($\overline{\rm MS}$). So the momentum integrals are replaced by

$$\int \frac{d^3p}{(2\pi)^3} \to \int_p \equiv \left(\frac{e^{\gamma_E} M^2}{4\pi}\right)^\epsilon \int \frac{d^dp}{(2\pi)^d} \; , \tag{A1}$$

where M is an arbitrary mass scale and $\gamma_E \simeq 0.5772$ is the Euler-Mascheroni constant. Very often, in evaluating the contributions to $\langle\phi^2\rangle_u$ one considers the integral

$$\int_p \frac{1}{(p^2+\eta^2)^n} = \frac{\eta^{3-2n}}{(4\pi)^{3/2}} \frac{\Gamma[n+\epsilon-3/2]}{\Gamma(n)} \left(\frac{M^2 e^{\gamma_E}}{\eta^2}\right)^\epsilon \; . \tag{A2}$$

This integral can be explicitly evaluated as above or by considering the case $n = 1$

$$\begin{aligned} \int_p \frac{1}{p^2+\eta^2} &= -\frac{\eta}{4\pi}\left\{1 + \epsilon\left[2\ln\left(\frac{M}{\eta}\right) + 2 - \ln(4)\right]\right. \\ &+ \left.\epsilon^2\left[4 + \frac{\pi^2}{4} + 2\ln^2\left(\frac{M}{2\eta}\right) + 4\ln\left(\frac{M}{2\eta}\right)\right] + \mathcal{O}(\epsilon^3)\right\} \; , \end{aligned} \tag{A3}$$

and its derivatives with respect to η^2:

$$\int_p \frac{1}{(p^2+\eta^2)^n} = \frac{1}{(n-1)!}\left(-\frac{d}{d\eta^2}\right)^{n-1} \int_p \frac{1}{p^2+\eta^2} \; . \tag{A4}$$

Let us now consider the three-loop contributions to $\langle\phi^2\rangle_u$ with any number of, external and/or internal, $\delta\eta^2$ insertions. Their general form is

$$(\delta\eta^2)^{n-2} N \int_p \frac{\delta^c \Sigma_a(p)}{(p^2+\eta^2)^n} \; , \tag{A5}$$

where c is defined below and n determines the number of external (to the setting sun) $\delta\eta^2$ insertions. At the same time the insertions, internal to the setting sun, are taken into account by

$$\Sigma_a(p) = -\frac{\mathcal{M}(N+2)}{18} u^2 \int_{kq} \frac{1}{(k^2+\eta^2)^m} \frac{(\delta\eta^2)^{m+j+h-3}}{(q^2+\eta^2)^j} \frac{1}{[(p+k+q)^2+\eta^2]^h} \; , \tag{A6}$$

where $\mathcal{M}$ defines the multiplicity of equivalent internal $\delta\eta^2$ insertions. This general contribution to $\langle\phi^2\rangle_u$ can be written as

$$\begin{aligned} -(\delta\eta^2)^{n-2} N \int_p \frac{\delta^c \Sigma_a(p)}{(p^2+\eta^2)^n} &= \delta^{n+m+j+h-3} \frac{N(N+2)\mathcal{M}}{18} u^2 (\eta^2)^{n+m+j+h-5} \\ &\times \int_{pkq} \frac{1}{(p^2+\eta^2)^n} \frac{1}{(k^2+\eta^2)^m} \frac{1}{(q^2+\eta^2)^j} \frac{1}{[(p+k+q)^2+\eta^2]^h} \; , \end{aligned} \tag{A7}$$

where $c = m + j + h - 1$ labels the order of the two-loop (setting sun) self-energy term. Now, we can merge all propagators through the use of standard Feynman parametrization, given as usual by

$$\frac{1}{a^x b^y} = \frac{\Gamma[x+y]}{\Gamma[x]\Gamma[y]} \int_0^1 d\alpha \frac{\alpha^{x-1}(1-\alpha)^{y-1}}{[a\alpha + b(1-\alpha)]^{x+y}} \; , \quad (x, y > 0) \; . \tag{A8}$$

or other generalizations. One then gets

$$\begin{aligned}(\delta\eta^2)^{n-2} N \int_p \frac{\delta^c \Sigma_a(p)}{(p^2+\eta^2)^n} &= -\frac{\delta^{n+m+j+h-3}}{(4\pi)^{9/2}} \frac{N(N+2)\mathcal{M}}{18} \frac{u^2}{\eta} \frac{\Gamma[n+m+j+h-9/2+3\epsilon]}{\Gamma[n]\Gamma[m]\Gamma[j]\Gamma[h]} \\ &\times \left(\frac{e^{\gamma_E} M^2}{\eta^2}\right)^{3\epsilon} \int_0^1 d\alpha d\beta d\gamma \frac{g(\alpha)g(\beta)g(\gamma)}{[g(\alpha,\beta,\gamma)]^{n+m+j+h-9/2+3\epsilon}} \; ,\end{aligned} \tag{A9}$$

where

$$g(\alpha) = \alpha^{j-1}(1-\alpha)^{h-1}[\alpha(1-\alpha)]^{-j-h+3/2-\epsilon} \; , \tag{A10}$$

$$g(\beta) = \beta^{m-1}(1-\beta)^{j+h-5/2+\epsilon}[\beta(1-\beta)]^{-j-h-m+3-2\epsilon} \; , \tag{A11}$$

$$g(\gamma) = \gamma^{n-1}(1-\gamma)^{j+h+m-4+2\epsilon} \; , \tag{A12}$$

and

$$g(\alpha,\beta,\gamma) = \gamma + \frac{1-\gamma}{1-\beta} + \frac{1-\gamma}{\beta\alpha(1-\alpha)} \; . \tag{A13}$$

Then, for given n, m, j and h one performs the expansion in ϵ keeping the poles and finite terms as usual. For most situations found in the present work the integrals over the Feynman parameters need to be evaluated numerically. Here we use Monte Carlo and Vegas techniques to perform those integrations. We have taken particular care to keep the numerical errors less than approximately 1% in our final numerical results.

One must be careful in carrying out the ϵ expansion in the expression above since sometimes the divergences can be hidden on the exponents of the Feynman parameters. Since m, n, j and h are positive integers ($n \geq 2$, $m, j, h \geq 1$) one sees that $g(\gamma)$ has a pole as $\epsilon \to 0$ when $j = h = m = 1$ corresponding to a setting sun diagram without internal $\delta\eta^2$ insertions. This is the only situation where one has ultraviolet divergences for these contributions. For $j = h = m = 1$ the actual divergence appears in the term $(1-\gamma)^{2\epsilon-1}$ contained in $g(\gamma)$ and it will appear as a $1/\epsilon$ pole if one integrates

$$\int_0^1 d\gamma \frac{g(\gamma)}{[g(\alpha,\beta,\gamma)]^{n+m+j+h-9/2+3\epsilon}} \; , \tag{A14}$$

by parts. The case $p = 0$ follows essentially the same lines and the general result for the setting sun type of contribution with any internal and/or external $\delta\eta^2$ insertions is

$$\begin{aligned}(\delta\eta^2)^{n-2} N \int_p \frac{\delta^c \Sigma_a(0)}{(p^2+\eta^2)^n} &= -\frac{\delta^{n+m+j+h-3}}{(4\pi)^3} \frac{N(N+2)\mathcal{M}}{18} u^2 (\eta^2)^{n-2} \frac{\Gamma[m+j+h-3+2\epsilon]}{\Gamma[m]\Gamma[j]\Gamma[h]} \\ &\times \left(\frac{e^{\gamma_E} M^2}{\eta^2}\right)^{2\epsilon} \int_0^1 d\alpha d\beta \frac{g(\alpha)g(\beta)}{[g(\alpha,\beta)]^{m+j+h-3+2\epsilon}} \int_p \frac{1}{(p^2+\eta^2)^n} \; ,\end{aligned} \tag{A15}$$

where the integral over p can be readily obtained by one of the methods discussed in the beginning of this appendix and

$$g(\alpha,\beta)=\frac{1}{1-\beta}+\frac{1}{\beta\alpha(1-\alpha)}\ . \tag{A16}$$

Note that the gamma function in Eq. (A15) displays an ultraviolet pole when $m=j=h=1$ and is finite otherwise.

The first contribution (sixth diagram of Fig. 3) of this type appears at $\mathcal{O}(\delta^2)$ with $n=2, m=j=h=1$. Since there is just one graph like this, $\mathcal{M}=1$, and one writes

$$-N\int_p\frac{\delta^2\Sigma_1(p)}{(p^2+\eta^2)^2}=\delta^2\frac{N(N+2)}{18(4\pi)^3}\frac{u^2}{\eta}\left[\frac{1}{\epsilon}+6\ln\left(\frac{M}{\eta}\right)-4.93147\right]\ . \tag{A17}$$

The $p=0$ contribution is given by

$$N\int_p\frac{\delta^2\Sigma_1(0)}{(p^2+\eta^2)^2}=-\delta^2\frac{N(N+2)}{18(4\pi)^3}\frac{u^2}{\eta}\left[\frac{1}{\epsilon}+6\ln\left(\frac{M}{\eta}\right)-3.78069\right]\ . \tag{A18}$$

The last two equations reproduce the results found analytically by Braaten and Nieto in Ref. [38]. Note that although Eq. (A17) and Eq. (A18) diverge, their sum is finite and scale independent. Together, they give the contribution

$$-N\int_p\frac{\delta^2[\Sigma_1(p)-\Sigma_1(0)]}{(p^2+\eta^2)^2}=-\delta^2\frac{u^2}{\eta}\frac{N(N+2)}{18(4\pi)^3}[0.143848]\ , \tag{A19}$$

which is exactly the result found in our previous work, Ref. [4]. Now, we turn to the evaluation the setting suns with insertions. The most expedient way would be to do the replacement $\eta\to\eta(1-\delta)^{1/2}$ and then expand the squared root to the desired order. However, this procedure would only give the total contribution at each order. In order to have absolute control about each single contribution we prefer to use our general expressions Eqs. (A9) and (A15). We have checked both procedures finding that they agree to each other within 1% which is reassuring since when obtaining the diagrams with insertions via $\eta\to\eta(1-\delta)^{1/2}$ one has a result which may be considered exact since this expansion starts from Eq. (A19), and this result agrees with the analytical results of Refs. [4, 38]. Also, at order-δ^4, the general relations given by Eqs. (A9) and (A15) have proven to be very useful in the evaluation of diagrams containing the setting sun as insertion. For the eighth graph of figure 3 one has three cases similar to $n=m=2$ and $j=h=1$ ($\mathcal{M}=3$). This gives

$$-N\int_p\frac{\delta^3\Sigma_2(p)}{(p^2+\eta^2)^2}=\delta^3\frac{u^2}{\eta}\frac{N(N+2)}{18(4\pi)^3}[0.188]\ , \tag{A20}$$

and

$$N\int_p\frac{\delta^3\Sigma_2(0)}{(p^2+\eta^2)^2}=-\delta^3\frac{u^2}{\eta}\frac{N(N+2)}{18(4\pi)^3}[0.249]\ , \tag{A21}$$

which lead to

$$N\int_p\frac{\delta^3[\Sigma_2(p)-\Sigma_2(0)]}{(p^2+\eta^2)^2}=-\delta^3\frac{u^2}{\eta}\frac{N(N+2)}{18(4\pi)^3}[0.0610]\ . \tag{A22}$$

For the seventh graph of Fig. 3, $n=3$ and $m=h=j=1$ with $\mathcal{M}=1$, one has

$$-N\int_p\frac{\delta^3\eta^2\Sigma_1(p)}{(p^2+\eta^2)^3}=\delta^3\frac{u^2}{\eta}\frac{N(N+2)}{18(4\pi)^3}\frac{1}{32}\left[\frac{1}{\epsilon}+6\ln\left(\frac{M}{\eta}\right)-1.968\right]\ , \tag{A23}$$

and

$$N\int_p \frac{\delta^3\eta^2\Sigma_1(0)}{(p^2+\eta^2)^3} = -\delta^3\frac{u^2}{\eta}\frac{N(N+2)}{18(4\pi)^3}\frac{1}{32}\left[\frac{1}{\epsilon}+6\ln\left(\frac{M}{\eta}\right)-1.781\right]\,, \tag{A24}$$

which lead to

$$-N\int_p \frac{\delta^3\eta^2 2[\Sigma_1(p)-\Sigma_1(0)]}{(p^2+\eta^2)^3} = -\delta^3\frac{u^2}{\eta}\frac{N(N+2)}{18(4\pi)^3}[0.01168]\,. \tag{A25}$$

where the factor of 2 on the RHS accounts for the two possibilities of external insertions (see Eq. (4.2). For $n=4$ and $m=h=j=1$ (tenth diagram of Fig. 3) one gets, with $\mathcal{M}=1$,

$$-N\int_p \frac{\delta^4\eta^4\Sigma_1(p)}{(p^2+\eta^2)^4} = \delta^4\frac{N(N+2)}{18(4\pi)^3}\frac{1}{64}\frac{u^2}{\eta}\left[\frac{1}{\epsilon}+6\ln\left(\frac{M}{\eta}\right)-1.20111\right]\,, \tag{A26}$$

and

$$N\int_0 \frac{\delta^4\eta^4\Sigma_1(0)}{(p^2+\eta^2)^4} = -\delta^4\frac{N(N+2)}{18(4\pi)^3}\frac{1}{64}\frac{u^2}{\eta}\left[\frac{1}{\epsilon}+6\ln\left(\frac{M}{\eta}\right)-1.1408\right]\,, \tag{A27}$$

which leads to

$$-N\int_p \frac{3\delta^4\eta^4[\Sigma_1(p)-\Sigma_1(0)]}{(p^2+\eta^2)^4} = -\delta^4\frac{N(N+2)}{18(4\pi)^3}\frac{u^2}{\eta}[2.8270\times10^{-3}]\,, \tag{A28}$$

where the factor of 3 on the RHS accounts for the possibilities of external insertions (see Eq. (4.2). There are three cases ($\mathcal{M}=3$) similar to the case $n=3$, $m=2$ and $j=h=1$ displayed by the eleventh graph of Fig. 3. One gets

$$-N\int_p \frac{\delta^4\eta^2\Sigma_2(p)}{(p^2+\eta^2)^3} = \delta^4\frac{N(N+2)}{18(4\pi)^3}\frac{u^2}{\eta}[0.0586]\,, \tag{A29}$$

and

$$N\int_0 \frac{\delta^4\eta^2\Sigma_2(0)}{(p^2+\eta^2)^3} = -\delta^4\frac{N(N+2)}{18(4\pi)^3}\frac{u^2}{\eta}[0.0650]\,, \tag{A30}$$

which lead to

$$-N\int_p \frac{\delta^4\eta^2[2\Sigma_2(p)-\Sigma_2(0)]}{(p^2+\eta^2)^3} = -\delta^4\frac{N(N+2)}{18(4\pi)^3}\frac{u^2}{\eta}[7.7318\times10^{-3}]\,. \tag{A31}$$

The twelveth graph of Fig. 3 has $\mathcal{M}=3$, $n=2$, $m=3$ and $j=h=1$ leading to

$$-N\int_p \frac{\delta^4\Sigma_4(p)}{(p^2+\eta^2)^2} = \delta^4\frac{N(N+2)}{18(4\pi)^3}\frac{u^2}{\eta}[0.058638]\,, \tag{A32}$$

and

$$N\int_p \frac{\delta^4\Sigma_4(0)}{(p^2+\eta^2)^2} = -\delta^4\frac{N(N+2)}{18(4\pi)^3}\frac{u^2}{\eta}[0.083246]\,, \tag{A33}$$

which give

$$- N \int_p \frac{[\Sigma_4(p) - \Sigma_4(0)]}{(p^2+\eta^2)^2} = -\delta^4 \frac{N(N+2)}{18(4\pi)^3} \frac{u^2}{\eta} [0.02461] \, . \tag{A34}$$

Finally, for the thirteenth graph, $\mathcal{M} = 3$, $n = m = j = 2$ and $h = 1$ from which one gets

$$- N \int_p \frac{\delta^4 \Sigma_7(p)}{(p^2+\eta^2)^2} = \delta^4 \frac{N(N+2)}{18(4\pi)^3} \frac{u^2}{\eta} [0.0234552] \, , \tag{A35}$$

and

$$N \int_p \frac{\delta^4 \Sigma_7(0)}{(p^2+\eta^2)^2} = -\delta^4 \frac{N(N+2)}{18(4\pi)^4} \frac{u^2}{\eta} [0.0417] \, , \tag{A36}$$

which gives

$$- N \int_p \frac{\delta^4 [\Sigma_7(p) - \Sigma_7(0)]}{(p^2+\eta^2)^2} = -\delta^4 \frac{N(N+2)}{18(4\pi)^3} \frac{u^2}{\eta} [0.01825] \, . \tag{A37}$$

Let us now consider a general four-loop contribution with any number of internal and/or external $\delta\eta^2$ insertions. After performing few shifts on the integration variables one gets

$$\begin{aligned} - (\delta\eta^2)^{n-2} N \int_p \frac{\delta^d \Sigma_b(p)}{(p^2+\eta^2)^n} &= -\delta^{n+m+l+h+i+j-4} u^3 N \frac{\mathcal{M}\left(16+10N+N^2\right)}{108} (\eta^2)^{n+m+l+h+i+j-7} \\ &\times \int_{pqkt} \frac{1}{(t^2+\eta^2)^n (q^2+\eta^2)^m (k^2+\eta^2)^l [(p+q)^2+\eta^2]^h} \\ &\times \frac{1}{[(p+k)^2+\eta^2]^i [(p+t)^2+\eta^2]^j} \, , \end{aligned} \tag{A38}$$

where $d = m + l + h + i + j - 2$ labels the order of the three-loop self-energy term. Then, proceeding as in the three loop case one finds

$$\begin{aligned} - (\delta\eta^2)^{n-2} N \int_p \frac{\delta^d \Sigma_b(p)}{(p^2+\eta^2)^n} &= -N \frac{\delta^{n+m+l+h+i+j-4}}{(4\pi)^6} \frac{u^3}{\eta^2} \frac{\mathcal{M}\left(16+10N+N^2\right)}{108} \left(\frac{M^2 \exp\gamma_E}{\eta^2} \right)^{4\epsilon} \\ &\times \frac{\Gamma(n+m+l+h+i+j-6+4\epsilon)}{\Gamma(n)\Gamma(m)\Gamma(l)\Gamma(h)\Gamma(i)\Gamma(j)} \\ &\times \int_0^1 d\alpha d\beta d\gamma d\theta d\phi \frac{f(\alpha) f(\beta) f(\gamma) f(\theta) f(\phi)}{[f(\alpha,\beta,\gamma,\theta,\phi)]^{l+i+m+h+n+j-6+4\epsilon}} \, , \end{aligned} \tag{A39}$$

where

$$f(\alpha) = \alpha^{1/2-i-\epsilon} (1-\alpha)^{1/2-l-\epsilon} \, , \tag{A40}$$

$$f(\beta) = \beta^{1/2-h-\epsilon} (1-\beta)^{1/2-m-\epsilon} \, , \tag{A41}$$

$$f(\gamma) = \gamma^{1/2-j-\epsilon} (1-\gamma)^{1/2-n-\epsilon} \, , \tag{A42}$$

$$f(\theta) = \theta^{m+h-5/2+\epsilon} (1-\theta)^{n+j-5/2+\epsilon} \, , \tag{A43}$$

$$f(\phi) = \phi^{l+i-5/2+\epsilon}(1-\phi)^{n+j+m+h-4+2\epsilon} \; , \tag{A44}$$

and

$$f(\alpha,\beta,\gamma,\theta,\phi) = \frac{\phi}{\alpha(1-\alpha)} + \frac{\theta(1-\phi)}{\beta(1-\beta)} + \frac{(1-\theta)(1-\phi)}{\gamma(1-\gamma)} \; . \tag{A45}$$

As far as renormalization is concerned one should note that those type of four-loop contributions are always finite. The four-loop contribution whose self-energy has zero external momentum reads

$$(\delta\eta^2)^{n-2} N \int_p \frac{\delta^d \Sigma_b(0)}{(p^2+\eta^2)^n} \; , \tag{A46}$$

where

$$\begin{aligned} \Sigma_b(0) &= N\delta^3 u^3 \frac{\mathcal{M}\left(16+10N+N^2\right)}{108} (\delta\eta^2)^{n-2} (\delta\eta^2)^{m+l+h+i+j-5} \\ &\times \int_{qkt} \frac{1}{(q^2+\eta^2)^j (k^2+\eta^2)^l (t^2+\eta^2)^h [(q+k)^2+\eta^2]^i [(q+t)^2+\eta^2]^m} \; . \end{aligned} \tag{A47}$$

Proceeding as above one gets

$$\begin{aligned} (\delta\eta^2)^{n-2} N \int_p \frac{\delta^d \Sigma_b(0)}{(p^2+\eta^2)^n} &= \delta^{n+m+l+h+i+j-4} N \frac{u^3 (\eta^2)^{n-5/2}}{(4\pi)^{9/2}} \frac{\mathcal{M}\left(16+10N+N^2\right)}{108} \\ &\times \left(\frac{M^2 \exp\gamma_E}{\eta^2}\right)^{3\epsilon} \frac{\Gamma(m+l+h+i+j-9/2+3\epsilon)}{\Gamma(m)\Gamma(l)\Gamma(h)\Gamma(i)\Gamma(j)} \\ &\times \int_0^1 d\alpha d\beta d\gamma d\theta \frac{\gamma f(\alpha) f(\beta) f(\gamma,\theta)}{[f(\alpha,\beta,\gamma,\theta)]^{l+i+m+h+j-9/2+3\epsilon}} \\ &\times \int_p \frac{1}{(p^2+\eta^2)^n} \; , \end{aligned} \tag{A48}$$

where $f(\alpha)$ and $f(\beta)$ are given by Eqs. (A40) and (A41). Also, one has

$$f(\gamma,\theta) = (1-\gamma)^{j-1} [\gamma(1-\theta)]^{l+i+\epsilon-5/2} (\gamma\theta)^{h+m-5/2+\epsilon} \; , \tag{A49}$$

and

$$f(\alpha,\beta,\gamma,\theta) = (1-\gamma) + \frac{\gamma(1-\theta)}{\alpha(1-\alpha)} + \frac{\gamma\theta}{\beta(1-\beta)} \; . \tag{A50}$$

The first four-loop contribution of this type appears at order-δ^3 and is displayed by the ninth graph of Fig. 3 and it has $n=2$, $m=l=h=i=j=1$ and $\mathcal{M}=1$. The contributions to $\langle\phi^2\rangle_u$ are given by

$$-\delta^3 N \int_p \frac{\Sigma_3(p)}{(p^2+\eta^2)^2} = -\delta^3 \frac{u^3}{\eta^2} \frac{N}{(4\pi)^6} \frac{\left(16+10N+N^2\right)}{108} [32.4388] \; , \tag{A51}$$

and

$$\delta^3 N \int_p \frac{\Sigma_3(0)}{(p^2+\eta^2)^2} = \delta^3 \frac{u^3}{\eta^2} \frac{N}{(4\pi)^6} \frac{\left(16+10N+N^2\right)}{108} [40.538] \; , \tag{A52}$$

which lead to

$$-\delta^3 N\int_p \frac{[\Sigma_3(p)-\Sigma_3(0)]}{(p^2+\eta^2)^2}=\delta^3\frac{u^3}{\eta^2}\frac{N}{(4\pi)^6}\frac{\left(16+10N+N^2\right)}{108}[8.09927]\,. \tag{A53}$$

As for the three-loop case one could use the equation above to obtain a series expansion which would give the total contribution of graphs with insertions to any order in δ. However, we prefer to perform the individual evaluation of each contribution in order to achieve more control over the series expansion. At order-δ^4 the first contribution is displayed by the fourteenth graph with $\mathcal{M}=1$, $n=3$ and $m=l=h=i=j=1$. One then obtains

$$-\delta^4 N\int_p \frac{\eta^2\Sigma_3(p)}{(p^2+\eta^2)^3}=-\delta^4\frac{u^3}{\eta^2}\frac{N}{(4\pi)^6}\frac{\left(16+10N+N^2\right)}{108}[9.70448]\,, \tag{A54}$$

and

$$\delta^4 N\int_p \frac{\eta^2\Sigma_3(0)}{(p^2+\eta^2)^3}=\delta^4\frac{u^3}{\eta^2}\frac{N}{(4\pi)^6}\frac{\left(16+10N+N^2\right)}{108}[10.1344]\,, \tag{A55}$$

which lead to

$$-\delta^4 N\int_p \frac{2\eta^2[\Sigma_3(p)-\Sigma_3(0)]}{(p^2+\eta^2)^3}=\delta^4\frac{u^3}{\eta^2}\frac{N}{(4\pi)^6}\frac{\left(16+10N+N^2\right)}{108}[0.85984]\,, \tag{A56}$$

where, once more, the factor of 2 accounts for the two possibilities of internal insertions in accordance with Eq. (4.2).

Next, let us consider the case illustrated by the fifteenth graph of Fig. 3, which has $\mathcal{M}=1$, $n=j=2$ and $h=i=l=m=1$. After evaluating the integrals one gets

$$-\delta^4 N\int_p \frac{\Sigma_{10}(p)}{(p^2+\eta^2)^2}=-\delta^4\frac{u^3}{\eta^2}\frac{N}{(4\pi)^6}\frac{\left(16+10N+N^2\right)}{108}[3.18221]\,, \tag{A57}$$

and

$$\delta^4 N\int_p \frac{\Sigma_{10}(0)}{(p^2+\eta^2)^2}=\delta^4\frac{u^3}{\eta^2}\frac{N}{(4\pi)^6}\frac{\left(16+10N+N^2\right)}{108}[5.120]\,, \tag{A58}$$

which lead to

$$-\delta^4 N\int_p \frac{[\Sigma_{10}(p)-\Sigma_{10}(0)]}{(p^2+\eta^2)^2}=\delta^4\frac{u^3}{\eta^2}\frac{N}{(4\pi)^6}\frac{\left(16+10N+N^2\right)}{108}[1.9784]\,. \tag{A59}$$

The remaining four-loop contributions to this order are evaluated using the case displayed by the sixteenth diagram of Fig. 3 which has $\mathcal{M}=4$, $n=m=2$, $l=h=i=j=1$ and whose result is given by

$$-N\int_p \frac{\delta^4\Sigma_5(p)}{(p^2+\eta^2)^2}=-\delta^4\frac{u^3}{\eta^2}\frac{N}{(4\pi)^6}\frac{\left(16+10N+N^2\right)}{108}[9.85072]\,, \tag{A60}$$

and

$$N\int_p \frac{\delta^4\Sigma_5(0)}{(p^2+\eta^2)^2}=\delta^4\frac{u^3}{\eta^2}\frac{N}{(4\pi)^6}\frac{\left(16+10N+N^2\right)}{108}[15.15548]\,, \tag{A61}$$

which lead to

$$- N \int_p \frac{\delta^4[\Sigma_5(p) - \Sigma_5(0)]}{(p^2+\eta^2)^2} = \delta^4 \frac{u^3}{\eta^2} \frac{N}{(4\pi)^6} \frac{\left(16 + 10N + N^2\right)}{108} [5.30476] \; . \tag{A62}$$

Let us now consider the five-loop contributions. The first one is given by the seventeenth graph of Fig. 3,

$$\delta^4 N \int_p \frac{[\Sigma_1(p) - \Sigma_1(0)]^2}{(p^2+\eta^2)^3} = -\delta^4 \frac{u^4}{\eta^3} \frac{N(N+2)^2}{(18)^2 (4\pi)^7} [0.87339] \; , \tag{A63}$$

where the individual contributions are given by three terms starting with

$$\begin{aligned}
\delta^4 N \int_p \frac{[\Sigma_1(p)]^2}{(p^2+\eta^2)^3} &= \delta^4 \frac{u^4}{\eta^3} \frac{N(N+2)^2 \Gamma(3/2+5\epsilon)}{(18)^2 \Gamma(3) (4\pi)^{15/2}} \left(\frac{M^2 \exp \gamma_E}{\eta^2} \right)^{5\epsilon} \\
&\times \int_0^1 d\alpha d\beta d\gamma d\theta d\phi d\chi \frac{h(\alpha) h(\beta) h(\gamma) h(\theta) h(\phi) h(\chi)}{[h(\alpha,\beta,\gamma,\theta,\phi,\chi)]^{3/2+5\epsilon}} \\
&\times \left\{ \frac{1}{\epsilon^2} \left[1 - \frac{3}{4} \frac{\phi h(\alpha,\beta,\gamma,\theta,\chi)}{h(\alpha,\beta,\gamma,\theta,\phi,\chi)} - \frac{9}{8} \frac{\phi\gamma[1-h(\alpha,\beta)]}{h(\alpha,\beta,\gamma,\theta,\phi,\chi)} \right.\right. \\
&+ \left.\left. \frac{15}{16} \frac{\phi^2 \gamma [1-h(\alpha,\beta)] h(\alpha,\beta,\gamma,\theta,\chi)}{[h(\alpha,\beta,\gamma,\theta,\phi,\chi)]^2} \right] \right. \\
&+ \frac{1}{\epsilon} \left[1 - \frac{5}{2} \frac{\phi h(\alpha,\beta,\gamma,\theta,\chi)}{h(\alpha,\beta,\gamma,\theta,\phi,\chi)} - \frac{18}{4} \frac{\phi\gamma[1-h(\alpha,\beta)]}{h(\alpha,\beta,\gamma,\theta,\phi,\chi)} \right. \\
&+ \left. \frac{40}{8} \frac{\phi^2 \gamma [1-h(\alpha,\beta)] h(\alpha,\beta,\gamma,\theta,\chi)}{[h(\alpha,\beta,\gamma,\theta,\phi,\chi)]^2} \right] \\
&- \left. \frac{5}{2} \frac{\phi\gamma[1-h(\alpha,\beta)]}{h(\alpha,\beta,\gamma,\theta,\phi,\chi)} + \frac{25}{4} \frac{\phi^2 \gamma [1-h(\alpha,\beta)] h(\alpha,\beta,\gamma,\theta,\chi)}{[h(\alpha,\beta,\gamma,\theta,\phi,\chi)]^2} \right\} \; ,
\end{aligned} \tag{A64}$$

where

$$h(\alpha) = [\alpha(1-\alpha)]^{-1/2-\epsilon} \; , \tag{A65}$$

$$h(\beta) = (1-\beta)^{-1/2+\epsilon} [\beta(1-\beta)]^{-2\epsilon} \; , \tag{A66}$$

$$h(\gamma) = \gamma (1-\gamma)^{2\epsilon} \; , \tag{A67}$$

$$h(\theta) = [\theta(1-\theta)]^{-1/2-\epsilon} \; , \tag{A68}$$

$$h(\phi) = \phi^{1+2\epsilon} (1-\phi)^{2\epsilon} \; , \tag{A69}$$

$$h(\chi) = (1-\chi)^{-1/2+\epsilon} [\chi(1-\chi)]^{-2\epsilon} \; , \tag{A70}$$

$$h(\alpha,\beta) = \frac{1}{1-\beta} + \frac{1}{\beta\alpha(1-\alpha)} \; , \tag{A71}$$

$$h(\theta,\chi)=\frac{1}{1-\chi}+\frac{1}{\chi\theta(1-\theta)}\,, \tag{A72}$$

$$h(\alpha,\beta,\gamma,\theta,\chi)=\gamma-h(\theta,\chi)+(1-\gamma)h(\alpha,\beta)\,, \tag{A73}$$

and

$$h(\alpha,\beta,\gamma,\theta,\phi,\chi)=\gamma\phi+(1-\phi)h(\theta,\chi)+\phi(1-\gamma)h(\alpha,\beta)\,. \tag{A74}$$

After performing the expansion in ϵ and integrating numerically one obtains

$$\begin{aligned}\delta^4 N\int_p\frac{[\Sigma_1(p)]^2}{(p^2+\eta^2)^3} &= \delta^4\frac{u^4}{\eta^3}\frac{N(N+2)^2}{1296(8\pi)^5}\left\{\frac{1}{\epsilon^2}\right.\\ &+\left.\frac{1}{\epsilon}\left[10\ln\left(\frac{M}{\eta}\right)-4.419\right]+50\ln^2\left(\frac{M}{\eta}\right)-(44.19)\ln\left(\frac{M}{\eta}\right)+20.0158\right\}\,.\end{aligned} \tag{A75}$$

Now, expanding Eq. (A9), with $n=3, m=j=h=1$ to order ϵ and considering

$$\Sigma_1(0)=-\delta^2\frac{u^2}{(8\pi)^2}\frac{(N+2)}{18}\left\{\frac{1}{\epsilon}+4\ln\left(\frac{M}{\eta}\right)-2.3911+\epsilon\left[8\ln^2\left(\frac{M}{\eta}\right)+\frac{\pi^2}{3}-9.5644\ln\left(\frac{M}{\eta}\right)+4.3127\right]\right\}\,, \tag{A76}$$

one gets

$$\begin{aligned}-2\delta^4 N\int_p\frac{[\Sigma_1(p)\times\Sigma_1(0)]}{(p^2+\eta^2)^3} &= -\delta^4\frac{u^4}{\eta^3}\frac{N(N+2)^2}{648(8\pi)^5}\left\{\frac{1}{\epsilon^2}\right.\\ &+\left.\frac{1}{\epsilon}\left[10\ln\left(\frac{M}{\eta}\right)-4.3067\right]+50\ln^2\left(\frac{M}{\eta}\right)-(42.937)\ln\left(\frac{M}{\eta}\right)+18.9756\right\}\,.\end{aligned} \tag{A77}$$

The final contribution to this diagram is obtained by considering Eq. (A2), with $n=3$, expanded to order ϵ^2 and by taking the square of Eq. (A76) which leads to

$$\begin{aligned}\delta^4 N\int_p\frac{[\Sigma_1(0)]^2}{(p^2+\eta^2)^3} &= \delta^4\frac{u^4}{\eta^3}\frac{N(N+2)^2}{1296(8\pi)^5}\left\{\frac{1}{\epsilon^2}\right.\\ &+\left.\frac{1}{\epsilon}\left[10\ln\left(\frac{M}{\eta}\right)-4.1684\right]+50\ln^2\left(\frac{M}{\eta}\right)-(41.684)\ln\left(\frac{M}{\eta}\right)+18.6434\right\}\,.\end{aligned} \tag{A78}$$

Next, let us consider the eighteenth graph of Fig. 3 whose contribution comes from

$$\begin{aligned}-\delta^4 N\int_p\frac{\Sigma_6(p)}{(p^2+\eta^2)^2} &= \delta^4\frac{u^4}{\eta^3}\frac{N}{(4\pi)^{15/2}}\frac{\left(40+32N+8N^2+N^3\right)}{648}\Gamma(3/2+5\epsilon)\left(\frac{M^2\exp\gamma_E}{\eta^2}\right)^{5\epsilon}\\ &\times\int_0^1 d\alpha d\beta d\gamma d\theta d\phi d\chi d\zeta\frac{y(\alpha)y(\beta)y(\gamma)y(\theta)y(\phi)y(\chi)y(\zeta)}{[y(\alpha,\beta,\gamma,\theta,\phi,\chi,\zeta)]^{3/2+5\epsilon}}\,.\end{aligned} \tag{A79}$$

where

$$y(\alpha)=\alpha[\alpha(1-\alpha)]^{-3/2-\epsilon}\,, \tag{A80}$$

$$y(\beta)=[\beta(1-\beta)]^{-1/2-\epsilon}\,, \tag{A81}$$

$$y(\gamma) = [\gamma(1-\gamma)]^{-1/2-\epsilon} \; , \tag{A82}$$

$$y(\theta) = [\theta(1-\theta)]^{-1/2-\epsilon} \; , \tag{A83}$$

$$y(\phi) = \phi^{1/2+\epsilon}(1-\phi)^{-1/2+\epsilon} \; , \tag{A84}$$

$$y(\chi) = [\chi(1-\chi)]^{-1/2+\epsilon} \; , \tag{A85}$$

$$y(\zeta) = \zeta^{1+2\epsilon}(1-\zeta)^{2\epsilon} \; , \tag{A86}$$

and

$$y(\alpha,\beta,\gamma,\theta,\phi,\chi,\zeta) = \frac{\zeta(1-\phi)}{\beta(1-\beta)} + \frac{\phi\zeta}{\alpha(1-\alpha)} + \frac{(1-\chi)(1-\zeta)}{\theta(1-\theta)} + \frac{\chi(1-\zeta)}{\gamma(1-\gamma)} \; . \tag{A87}$$

This contribution is finite and yields

$$-\delta^4 N \int_p \frac{\Sigma_6(p)}{(p^2+\eta^2)^2} \;=\; \delta^4 \frac{u^4}{\eta^3}\frac{N}{(4\pi)^7}\frac{\left(40+32N+8N^2+N^3\right)}{648}[7.05619233] \; . \tag{A88}$$

The $p=0$ case is given by

$$\begin{aligned}\delta^4 N \int_p \frac{\Sigma_6(0)}{(p^2+\eta^2)^2} \;&=\; -\delta^4 \frac{u^4}{\eta^2}\frac{N}{(4\pi)^6}\frac{\left(40+32N+8N^2+N^3\right)}{648}\Gamma(1+4\epsilon)\left(\frac{M^2\exp\gamma_E}{\eta^2}\right)^{4\epsilon} \\ &\times \int_0^1 d\alpha d\beta d\gamma d\theta d\phi d\chi \frac{y\prime(\alpha)y(\beta)y(\gamma)y\prime(\theta)y\prime(\phi)y(\chi)}{[y(\alpha,\beta,\gamma,\theta,\phi,\chi)]^{1+4\epsilon}} \int_p \frac{1}{(p^2+\eta^2)^2} \; ,\end{aligned} \tag{A89}$$

where

$$y\prime(\alpha) = [\alpha(1-\alpha)]^{-1/2-\epsilon} \; , \tag{A90}$$

$$y\prime(\theta) = (1-\theta)^{-1/2+\epsilon} \; , \tag{A91}$$

$$y\prime(\phi) = \phi^{1/2+\epsilon}(1-\phi)^{2\epsilon} \; , \tag{A92}$$

$$y(\alpha,\beta,\gamma,\theta,\phi,\chi) = \phi\theta + \frac{\phi(1-\theta)}{\alpha(1-\alpha)} + \frac{\chi(1-\phi)}{\beta(1-\beta)} + \frac{(1-\chi)(1-\phi)}{\gamma(1-\gamma)} \; . \tag{A93}$$

Integrating one obtains

$$\delta^4 N \int_p \frac{\Sigma_6(0)}{(p^2+\eta^2)^2} \;=\; -\delta^4 \frac{u^4}{\eta^3}\frac{N}{(4\pi)^7}\frac{\left(40+32N+8N^2+N^3\right)}{648}[10.21524] \; . \tag{A94}$$

Together these contributions yield

$$-\delta^4 N\int_p \frac{[\Sigma_6(p)-\Sigma_6(0)]}{(p^2+\eta^2)^2} = -\delta^4\frac{u^4}{\eta^3}\frac{N}{(4\pi)^7}\frac{\left(40+32N+8N^2+N^3\right)}{648}[3.15904767]\,. \tag{A95}$$

The nineteenth contribution of Fig. 3 is given by

$$-N\int_p \frac{[\Sigma_8(p)-\Sigma_8(0)]}{(p^2+\eta^2)^2} = -\delta^4\frac{u^4}{\eta^3}\frac{N}{(4\pi)^7}\frac{\left(44+32N+5N^2\right)}{324}[1.70959]\,. \tag{A96}$$

The first contribution to this result follows from

$$\begin{aligned}-\delta^4 N\int_p \frac{\Sigma_8(p)}{(p^2+\eta^2)^2} \;&=\; \delta^4\frac{u^4}{\eta^3}\frac{N}{(4\pi)^{15/2}}\frac{\left(44+32N+5N^2\right)}{324}\Gamma(3/2+5\epsilon)\left(\frac{M^2\exp\gamma_E}{\eta^2}\right)^{5\epsilon}\\ &\times\int_0^1 d\alpha d\beta d\gamma d\theta d\phi d\chi d\xi\frac{k(\alpha)k(\beta)k(\theta)k(\phi)k(\chi)k(\gamma)k(\xi)k(\phi,\theta)\Lambda_8^{-3/2-3\epsilon}}{[1-\gamma+\Xi_8\gamma]^{3/2+5\epsilon}}\,,\end{aligned} \tag{A97}$$

where

$$k(\alpha)=[\alpha(1-\alpha)]^{-1/2-\epsilon}\,, \tag{A98}$$

$$k(\beta)=[\beta(1-\beta)]^{-1-4\epsilon}\beta^{1/2+3\epsilon}\,, \tag{A99}$$

$$k(\phi)=\phi^{-3/2-\epsilon}\,, \tag{A100}$$

$$k(\theta)=(1-\theta)^{-1/2-\epsilon}\,, \tag{A101}$$

$$k(\chi)=(1-\chi)^{1+2\epsilon}\,, \tag{A102}$$

$$k(\gamma)=(1-\gamma)\gamma^{4\epsilon}\,, \tag{A103}$$

$$k(\xi)=\xi^{2\epsilon}\,, \tag{A104}$$

$$k(\phi,\theta)=[1-\phi(1-\theta)]^{-1-2\epsilon}\,, \tag{A105}$$

$$\Lambda_8=\chi+\frac{\theta^2\xi(1-\chi)}{[1-\phi(1-\theta)]^2}-\left[\chi+\frac{\theta\xi(1-\chi)}{1-\phi(1-\theta)}\right]^2-\frac{\theta^2\xi(1-\chi)}{1-\phi(1-\theta)}+\frac{\xi(1-\chi)\theta(1-\theta)}{\phi(1-\theta)[1-\phi(1-\theta)]}\,, \tag{A106}$$

and

$$\Xi_8=\frac{1-\beta+\beta+\beta\,\Phi_8/\Lambda_8}{\beta(1-\beta)}\,, \tag{A107}$$

with

$$\Phi_8 = 1 - \xi(1-\chi) + \xi(1-\chi)\frac{1-\phi(1-\theta)+\frac{\phi(1-\theta)}{\alpha(1-\alpha)}}{\phi(1-\theta)[1-\phi(1-\theta)]} \; . \tag{A108}$$

Integrating one obtains

$$-\delta^4 N \int_p \frac{\Sigma_8(p)}{(p^2+\eta^2)^2} \;=\; \delta^4 \frac{u^4}{\eta^3}\frac{N}{(4\pi)^7}\frac{\left(44+32N+5N^2\right)}{324}[4.31098] \tag{A109}$$

The $p=0$ case is given by

$$\begin{aligned}\delta^4 N \int_p \frac{\Sigma_8(0)}{(p^2+\eta^2)^2} \;&=\; -\delta^4 \frac{u^4}{\eta^3}\frac{N}{(4\pi)^{15/2}}\frac{\left(44+32N+5N^2\right)}{324}\Gamma(1+4\epsilon)\Gamma(1/2+\epsilon)\left(\frac{M^2\exp\gamma_E}{\eta^2}\right)^{4\epsilon} \\ &\times \int_0^1 d\alpha d\beta d\xi d\theta d\phi d\chi \frac{k(\alpha)k(\beta)k(\xi)k(\theta)k(\phi)k(\chi)k(\phi,\theta)\Lambda_8^{-3/2-3\epsilon}}{\Xi_8^{1+4\epsilon}} \; ,\end{aligned} \tag{A110}$$

with the same notation as used in Eq. (A97). Integrating Eq. (A110) one obtains

$$\delta^4 N \int_p \frac{\Sigma_8(0)}{(p^2+\eta^2)^2} \;=\; -\delta^4 \frac{u^4}{\eta^3}\frac{N}{(4\pi)^7}\frac{\left(44+32N+5N^2\right)}{324}[6.02057] \; . \tag{A111}$$

We have another five-loop contribution given by the twentieth graph of Fig. 3 whose contribution is

$$-N\int_p \frac{[\Sigma_9(p)-\Sigma_9(0)]}{(p^2+\eta^2)^2} = -\delta^4\frac{u^4}{\eta^3}\frac{\mathcal{M}N(N+2)^2}{(18)^2(4\pi)^7}[1.4803] \; , \tag{A112}$$

where $\mathcal{M}=3$ accounts for the three possible ways of inserting one setting sun within another graph of the same type. The first term on the LHS of Eq. (A112) is

$$\begin{aligned}-\delta^4 N\int_p \frac{\Sigma_9(p)}{(p^2+\eta^2)^2} &= -\delta^4\frac{N(N+2)}{18}u^2\int_{pkq}\frac{1}{(p^2+\eta^2)^2}\frac{1}{(k^2+\eta^2)}\frac{[\Sigma_1(q)-\Sigma_1(0)]}{(q^2+\eta^2)^2}\frac{1}{[(p+k+q)^2+\eta^2]} \\ &= \delta^4\frac{u^4}{\eta^3}\frac{N(N+2)^2\Gamma(3/2+5\epsilon)}{(18)^2(4\pi)^{15/2}}\left(\frac{M^2\exp\gamma_E}{\eta^2}\right)^{5\epsilon}\int_0^1 d\alpha d\beta d\gamma d\theta d\phi d\chi \frac{x(\alpha)x(\beta)x(\gamma)x(\theta)x(\phi)x(\chi)}{[x(\alpha,\beta,\gamma,\theta,\phi,\chi)]^{3/2+5\epsilon}} \\ &\times\left\{\frac{1}{2\epsilon}\left[1-\frac{3}{2}\frac{x'(\alpha,\beta,\gamma,\theta,\phi,\chi)}{x(\alpha,\beta,\gamma,\theta,\phi,\chi)}\right]-\frac{5}{2}\frac{x'(\alpha,\beta,\gamma,\theta,\phi,\chi)}{x(\alpha,\beta,\gamma,\theta,\phi,\chi)}\right\} \\ &-\delta^4\frac{u^4}{\eta^3}\frac{N(N+2)^2}{(18)^2}\frac{[\pi\times 10^{-5}]}{(8\pi)^2}\left[\frac{1}{\epsilon}+10\ln\left(\frac{M}{\eta}\right)-5.9258\right] \; .\end{aligned} \tag{A113}$$

Note that $\Sigma_1(q)$ and $\Sigma_1(0)$ have, except for the labeling of momenta, the same form as Eqs. (A9) and (A15) with $m=j=h=1$. The x functions are given by

$$x(\alpha) = [\alpha(1-\alpha)]^{-1/2-\epsilon} \; , \tag{A114}$$

$$x(\beta) = (1-\beta)^{-1/2+\epsilon}[\beta(1-\beta)]^{-2\epsilon} \; , \tag{A115}$$

$$x(\gamma) = (1-\gamma)^{2\epsilon} \; , \tag{A116}$$

$$x(\theta) = \theta^{1+2\epsilon}[\theta(1-\theta)]^{-3/2-3\epsilon} \ , \tag{A117}$$

$$x(\phi) = (1-\phi)^{1/2+3\epsilon}[\phi(1-\phi)]^{-1-4\epsilon} \ , \tag{A118}$$

$$x(\chi) = \chi(1-\chi)^{4\epsilon} \ , \tag{A119}$$

$$x(\alpha,\beta) = \frac{1}{1-\beta} + \frac{1}{\beta\alpha(1-\alpha)} \ , \tag{A120}$$

$$x(\alpha,\beta,\gamma,\theta,\phi,\chi) = \chi + x(\alpha,\beta)\frac{(1-\gamma)(1-\chi)}{\phi(1-\theta)} + \frac{\gamma(1-\chi)}{\phi(1-\theta)} + \frac{(1-\chi)}{(1-\phi)} + \frac{(1-\chi)}{\theta\phi} \ , \tag{A121}$$

and

$$x'(\alpha,\beta,\gamma,\theta,\phi,\chi) = \frac{\gamma(1-\chi)}{\phi(1-\theta)}[1-x(\alpha,\beta)] \ . \tag{A122}$$

Then after integrating over the Feynman parameters and expanding in ϵ one gets

$$\begin{aligned} -\delta^4 N\int_p \frac{\Sigma_9(p)}{(p^2+\eta^2)^2} &= \delta^4\frac{u^4}{\eta^3}\frac{N(N+2)^2}{(18)^2}\frac{u^4}{\eta^3}\frac{[\pi\times 10^{-5}]}{(8\pi)^2}\left[\frac{1}{\epsilon}+10\ln\left(\frac{M}{\eta}\right)-6.83485\right] \\ &- \delta^4\frac{u^4}{\eta^3}\frac{N(N+2)^2}{(18)^2}\frac{u^4}{\eta^3}\frac{[\pi\times 10^{-5}]}{(8\pi)^2}\left[\frac{1}{\epsilon}+10\ln\left(\frac{M}{\eta}\right)-5.9258\right] \ , \end{aligned} \tag{A123}$$

which gives the finite, scale independent result

$$-\delta^4 N\int_p \frac{\Sigma_9(p)}{(p^2+\eta^2)^2} = -\delta^4\frac{u^4}{\eta^3}\frac{N(N+2)^2}{(18)^2}\frac{u^4}{\eta^3}\frac{[\pi\times 10^{-5}]}{(8\pi)^2}[0.90905] \ . \tag{A124}$$

The other contribution is given by

$$\begin{aligned} &\delta^4 N\int_p \frac{\Sigma_9(0)}{(p^2+\eta^2)^2} = \delta^4\frac{N(N+2)}{18}u^2\int_{pkq}\frac{1}{(p^2+\eta^2)^2}\frac{1}{(k^2+\eta^2)}\frac{[\Sigma_1(q)-\Sigma_1(0)]}{(q^2+\eta^2)^2}\frac{1}{[(k+q)^2+\eta^2]} \\ &= -\delta^4\frac{u^4}{\eta^2}\frac{N(N+2)^2\Gamma(1+4\epsilon)}{(18)^2(4\pi)^6}\left(\frac{M^2\exp\gamma_E}{\eta^2}\right)^{4\epsilon}\int_0^1 d\alpha d\beta d\gamma d\theta d\phi\frac{x(\alpha)x(\beta)x(\gamma)x(\theta)x(\phi)}{[x(\alpha,\beta,\gamma,\theta,\phi)]^{1+4\epsilon}} \\ &\times\left\{\frac{1}{2\epsilon}\left[1-\frac{x'(\alpha,\beta,\gamma,\theta,\phi)}{x(\alpha,\beta,\gamma,\theta,\phi)}\right]-2\frac{x'(\alpha,\beta,\gamma,\theta,\phi)}{x(\alpha,\beta,\gamma,\theta,\phi)}\right\}\int_p\frac{1}{(p^2+\eta^2)^2} \\ &+\delta^4\frac{u^4}{\eta^3}\frac{N(N+2)^2}{(18)^2}\frac{[4.1906\times 10^{-5}]}{(8\pi)^2}\left[\frac{1}{\epsilon}+10\ln\left(\frac{M}{\eta}\right)-6.17383\right] \ , \end{aligned} \tag{A125}$$

where

$$x(\alpha,\beta,\gamma,\theta,\phi) = x(\alpha,\beta)\frac{(1-\gamma)}{\phi(1-\theta)} + \frac{\gamma}{\phi(1-\theta)} + \frac{1}{\theta\phi} + \frac{1}{(1-\phi)} \ , \tag{A126}$$

and

$$x'(\alpha,\beta,\gamma,\theta,\phi) = \frac{\gamma}{\phi(1-\theta)}(1-x(\alpha,\beta)) \; . \tag{A127}$$

Integrating over the parameters and expanding one gets

$$\begin{aligned} \delta^4 N \int_p \frac{\Sigma_9(0)}{(p^2+\eta^2)^2} &= -\delta^4 \frac{u^4}{\eta^3}\frac{N(N+2)^2}{(18)^2}\frac{[4.1906\times 10^{-5}]}{(8\pi)^2}\left[\frac{1}{\epsilon}+10\ln\left(\frac{M}{\eta}\right)-6.40439\right] \\ &+ \delta^4 \frac{u^4}{\eta^3}\frac{N(N+2)^2}{(18)^2}\frac{[4.1906\times 10^{-5}]}{(8\pi)^2}\left[\frac{1}{\epsilon}+10\ln\left(\frac{M}{\eta}\right)-6.17383\right] \; , \end{aligned} \tag{A128}$$

which gives the finite, scale independent result

$$\delta^4 N \int_p \frac{\Sigma_9(0)}{(p^2+\eta^2)^2} = \delta^4 \frac{u^4}{\eta^3}\frac{N(N+2)^2}{(18)^2}\frac{[4.1906\times 10^{-5}]}{(8\pi)^2}[0.23056] \; . \tag{A129}$$

The final contribution comes from the last diagram of Fig. 3 and reads

$$-N\int_p \frac{[\Sigma_{11}(p)-\Sigma_{11}(0)]}{(p^2+\eta^2)^2} = -\delta^4\frac{u^4}{\eta^3}\frac{N}{(4\pi)^7}\frac{\left(44+32N+5N^2\right)}{324}[2.37741] \; . \tag{A130}$$

The first contribution to this result follows from

$$\begin{aligned} -\delta^4 N\int_p \frac{\Sigma_{11}(p)}{(p^2+\eta^2)^2} &= +\delta^4\frac{u^4}{\eta^3}\frac{N}{(4\pi)^{15/2}}\frac{\left(44+32N+5N^2\right)}{324}\Gamma(3/2+5\epsilon)\left(\frac{M^2\exp\gamma_E}{\eta^2}\right)^{5\epsilon} \\ &\times \int_0^1 d\alpha d\beta d\gamma d\theta d\phi d\chi d\xi \frac{z(\alpha)z(\beta)z(\theta)z(\phi)z(\chi)z(\gamma)z(\xi)z(\phi,\theta)\Lambda^{-1-4\epsilon}}{[\gamma+\frac{\Xi}{\Lambda}(1-\gamma)]^{3/2+5\epsilon}} \; , \end{aligned} \tag{A131}$$

where

$$z(\alpha) = [\alpha(1-\alpha)]^{-1/2-\epsilon} \; , \tag{A132}$$

$$z(\beta) = [\beta(1-\beta)]^{-1/2-\epsilon} \; , \tag{A133}$$

$$z(\phi) = \phi^{-1-2\epsilon}(1-\phi)^{-1/2+\epsilon} \; , \tag{A134}$$

$$z(\theta) = (1-\theta)^{-1/2-\epsilon} \; , \tag{A135}$$

$$z(\chi) = (1-\chi)^{1/2+3\epsilon} \; , \tag{A136}$$

$$z(\gamma) = \gamma(1-\gamma)^{4\epsilon} \; , \tag{A137}$$

$$z(\xi) = \xi^{2\epsilon}(1-\xi)^{-1/2+\epsilon} \; , \tag{A138}$$

$$z(\phi,\theta) = [1-\phi(1-\theta)]^{-1-2\epsilon} \ , \tag{A139}$$

$$\Lambda = \frac{\theta^2\xi(1-\chi)}{[1-\phi(1-\theta)]^2} + \chi - \left[\chi + \frac{\theta\xi(1-\chi)}{1-\phi(1-\theta)}\right]^2 + \Theta\xi(1-\chi) \ , \tag{A140}$$

$$\Xi = \frac{1-\chi-\xi(1-\chi)}{\beta(1-\beta)} + \chi + \Phi\xi(1-\chi) \ , \tag{A141}$$

with

$$\Theta = \frac{\theta(1-\theta)}{\phi(1-\theta)[1-\phi(1-\theta)]} + 1 + \frac{2\theta}{1-\phi(1-\theta)} - \frac{[1+\theta-\phi(1-\theta)]^2}{[1-\phi(1-\theta)]^2} \ , \tag{A142}$$

and

$$\Phi = \frac{1-\theta-\phi(1-\theta)}{\alpha(1-\alpha)\phi(1-\theta)[1-\phi(1-\theta)]} + \frac{\theta+\phi(1-\theta)}{\phi(1-\theta)[1-\phi(1-\theta)]} \ . \tag{A143}$$

Integrating, one obtains

$$-\delta^4 N \int_p \frac{\Sigma_{11}(p)}{(p^2+\eta^2)^2} \ = \ \delta^4 \frac{u^4}{\eta^3}\frac{N}{(4\pi)^7}\frac{\left(44+32N+5N^2\right)}{324}[6.12476] \quad . \tag{A144}$$

The $p=0$ case is given by

$$\begin{aligned}\delta^4 N \int_p \frac{\Sigma_{11}(0)}{(p^2+\eta^2)^2} \ &= \ -\delta^4 \frac{u^4}{\eta^3}\frac{N}{(4\pi)^{15/2}}\frac{\left(44+32N+5N^2\right)}{324}\Gamma(1+4\epsilon)\Gamma(1/2+\epsilon)\left(\frac{M^2\exp\gamma_E}{\eta^2}\right)^{4\epsilon} \\ &\times \ \int_0^1 d\alpha d\beta d\xi d\theta d\phi d\chi \frac{z(\alpha)z(\beta)z(\xi)z(\theta)z(\phi)z(\chi)z(\phi,\theta)}{\Xi^{1+4\epsilon}} \ ,\end{aligned} \tag{A145}$$

with the same notation as used in Eq. (A131). Integrating Eq. (A145) one obtains

$$\delta^4 N \int_p \frac{\Sigma_{11}(0)}{(p^2+\eta^2)^2} \ = \ -\delta^4 \frac{u^4}{\eta^3}\frac{N}{(4\pi)^7}\frac{\left(44+32N+5N^2\right)}{324}[8.50217] \ . \tag{A146}$$

---

[1] G. Baym, J.-P. Blaizot M. Holzmann, F. Laloë and D. Vautherin, Phys. Rev. Lett. **83**, 1703 (1999).
[2] G. Baym, J.-P. Blaizot and J. Zinn-Justin, Europhys. Lett. **49**, 150 (2000).
[3] P. Arnold and B. Tomásik, Phys. Rev. **A62**, 063604 (2000).
[4] F. F. de Souza Cruz, M. B. Pinto and R. O. Ramos, Phys. Rev. **B64**, 014515 (2001).
[5] P. Arnold and G. Moore, Phys. Rev. Lett. **87**, 120401 (2001); Phys. Rev. **E64**, 066113 (2001).
[6] V.A. Kashurnikov, N.V. Prokof'ev and B.V. Svistunov, Phys. Rev. Lett. **87**, 120402 (2001).
[7] M. Holzmann, G. Baym, J.-P. Blaizot and F. Laloë, Phys. Rev. Lett. **87**, 120403 (2001).
[8] P. Arnold, G. Moore and B. Tomásik, cond-mat/0107124.
[9] G. Baym, J.-P. Blaizot, M. Holzmann, F. Lalöe and D. Vautherin, cond-mat/0107129.
[10] J. Zinn-Justin, *Quantum Field Theroy and Critical Phenomena* (Oxford University Press, Oxford, England, 1996).
[11] S. Coleman, *Aspects of Symmetry* (Cambridge University Press, Cambridge, England, 1988).
[12] D.J. Gross and A. Neveu, Phys. Rev. **D10**, 3235 (1974).
[13] B. Rosenstein, B. Warr and S.H. Park; Phys. Rept. **205**, 59 (1991).
[14] A. Okopińska, Phys. Rev. **D35**, 1835 (1987).

[15] A. Duncan and M. Moshe, Phys. Lett. **B215**, 352 (1988).

[16] V.I. Yukalov, Mosc. Univ. Phys. Bull. **31**, 10 (1976); Teor. Mat. Fiz. **28**, 92 (1976); R. Seznec and J. Zinn-Justin, J. Math. Phys. **20**, 1398 (1979); J.C. LeGuillou and J. Zinn-Justin, Ann. Phys. **147**, 57 (1983).

[17] H. Kleinert, *Path Integrals in Quantum Mechanics, Statistics, Polymer Physics, and Financial Markets* (World Scientific Publishing Co., Singapore, 2001).

[18] P. M. Stevenson, Phys. Rev. **D23**, 2916 (1981).

[19] T. Hatsuda, T. Kunihiro and T. Tanaka, Phys. Rev. Lett. **78**, 3229 (1997); S. Chiku and T. Hatsuda, Phys. Rev. **D58**, 076001 (1998).

[20] P. Ramond *Field Theory: a Modern Primer* (Addison-Wesley Publ. Co., 1990).

[21] B. Bellet, P. Garcia and A. Neveu, Int. J. of Mod. Phys. **A11**, 5587 (1997); *ibid.* **A11**, 5607 (1997).

[22] I.R.C. Buckley, A. Duncan and H.F. Jones, Phys. Rev **D47**, 2554 (1993); A. Duncan and H.F. Jones, *ibid.* **D46**,2560 (1993); C.M. Bender, A. Duncan and H.F. Jones, *ibid.* **D49**, 4219 (1994); C. Arvanitis, H. F. Jones and C.S. Parker, *ibid.* **D52**, 3704 (1995).

[23] H. Kleinert and W. Janke, Phys. Lett. **A206**, 283 (1995).

[24] R. Guida, K. Konishi and H. Suzuki, Ann. Phys. **249**, 109 (1996).

[25] J.-L. Kneur and D. Reynaud, hep-th/0107073.

[26] C. M. Bender, K. Olausen and P. S. Wang, Phys. Rev. **D16**, 1780 (1977).

[27] G. Krein, D. P. Menezes and M.B. Pinto, Phys. Lett. **B370**, 5 (1996); G. Krein, D. P. Menezes and M.B. Pinto Int. J. of Mod. Phys. **E9**, 221 (2000).

[28] K. Banerjee, S.P. Bhatnagar, V. Choudry, S.S. Kandwal, Proc. R. Soc. Lond. **A 360**, 575 (1978).

[29] M. P. Blencowe and A. P. Korte, Phys. Rev. **B56**, 9422 (1997).

[30] M. B. Pinto and R. O. Ramos, Phys. Rev. **D60** , 105005 (1999).

[31] H. F. Jones, P. Parkin, Nucl. Phys. **B594**, 518 (2001).

[32] S. K. Gandhi and M. B. Pinto, Phys. Rev. **D49**, 4258 (1994).

[33] J.-L. Kneur, Phys. Rev. **D57**, 2785 (1998).

[34] R. Guida and J. Zinn-Justin, Nucl. Phys. **B489**, 626 (1997).

[35] M. B. Pinto and R. O. Ramos, Phys. Rev. **D61** 125016 (2000).

[36] D. Bedingham and T. S. Evans, Phys. Rev. **D64**, 105018 (2001).

[37] H. Kleinert, A. Pelster, B. Kastening and M. Bachmann, Phys. Rev **E62**, 1537 (2000); hep-th/0105193; H. Kleinert and V. Schulte-Frohlinde, *Critical Properties of* ϕ^4 *Theories* (World Scientific, Singapore, 2001); http://www.physik.fu-berlin.de/∼kleinert/294/programs.

[38] E. Braaten and A. Nieto, Phys. Rev. **D51**, 6990 (1995).

TABLE I: Comparision of the results for c_1 as obtained from different methods (see text) and at different orders of approximation.

MCLS	$1/N$ (LO)	$1/N$ NLO	SCR	$\mathcal{O}(\delta^2)$	$\mathcal{O}(\delta^3)$	$\mathcal{O}(\delta^4)$
~ 1.30	2.33	1.71	2.90	3.06	2.45	1.48

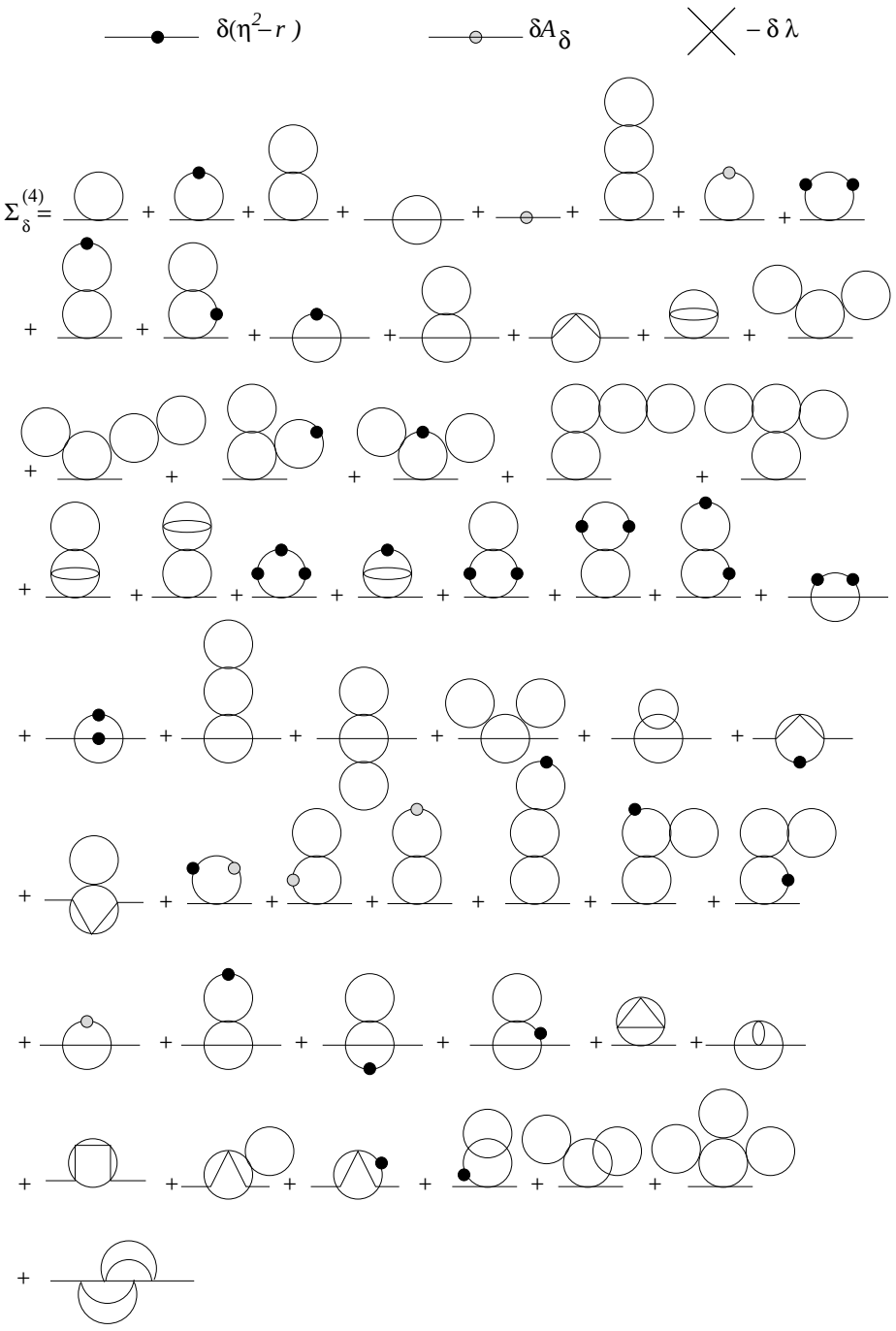

FIG. 1: Vertices (top) and diagrams contributing to the self-energy Σ_δ up to order δ^4.

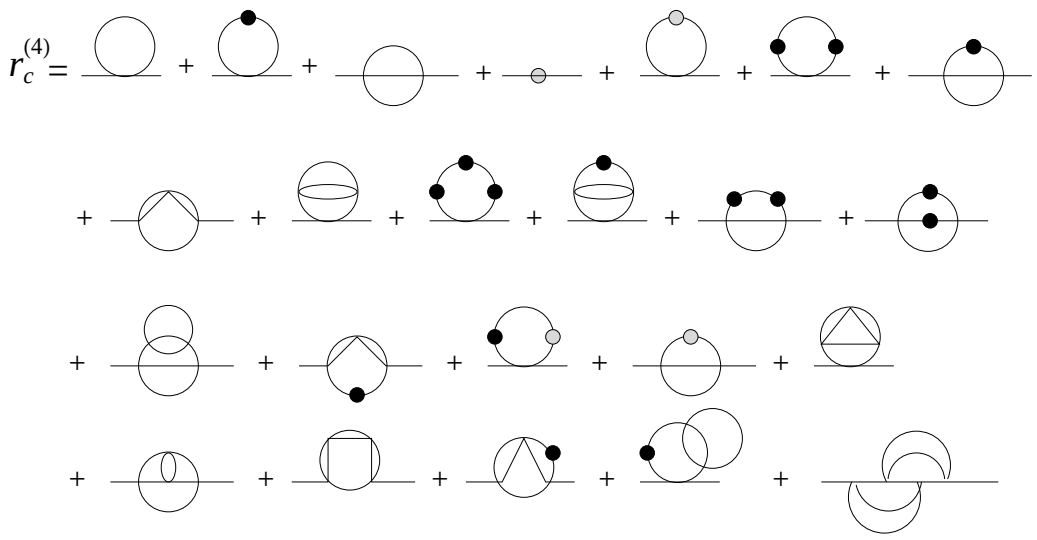

FIG. 2: The diagrams effectively contributing to r_c up to order δ^4. The black dot now represents only $\delta\eta^2$ insertions.

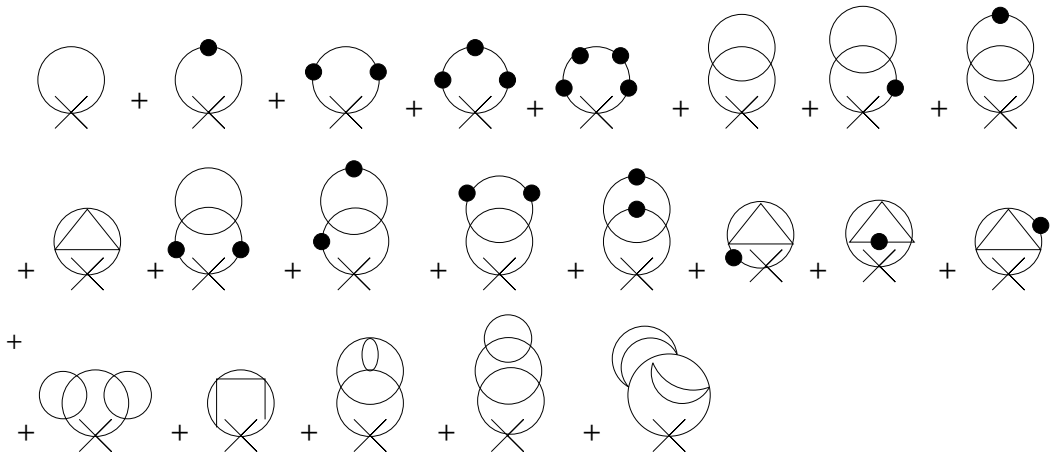

FIG. 3: All diagrams contributing to the two-point function $\langle\phi^2\rangle_\delta$, up to order δ^4, at the critical point. Again, the black dot represents here only the $\delta\eta^2$ insertions.